Reply to the reviewers for the manuscript:

"First forcing estimates from the future CMIP6 scenarios of anthropogenic aerosol optical properties and an associated Twomey effect" by Fiedler et al.

We would like to thank William Collins and the anonymous reviewer for their comments that helped improving our manuscript. In the following, we give our reply (blue) to each of the reviewer's comments (black) and document the associated changes in the manuscript.

Reviewer #1

Fiedler et al. present a modelling study in which they interpret the future emission scenarios of Riahi et al. (2017) using a simple model implemented in a GCM. The two aspects that provide added value compared to the Riahi et al. paper in my opinion are that geographical distributions are shown here, and that the scaling of Stevens et al. (2017) allows to convert the emissions into forcing values given the assumptions in the simple MACv2-SP approach (with some extra model information added from the simulated cloud fraction- and cloud droplet concentration distributions). As far as I understand, one of the co-authors, Gidden, prepares another manuscript for Geophys. Model Devel. that possibly covers the former aspect in a similar way.

Thank you for your comments. Matt Gidden, a co-author of this study, prepared another manuscript while we have developed our joint article. We cite his article in our article and update the reference and the names of the scenarios from his article in our revised manuscript. Our content substantially differs from that study. We here document the MACv2-SP interpretation of the CMIP6 scenarios and show the first forcing estimates for anthropogenic aerosol of the MACv2-SP interpretation of the CMIP6 emission scenarios.

The manuscript suffers from poor explanations. It is very difficult to follow the set-up of the simulations (e.g. number of years integrated, boundary conditions for these simulations).

We kept the description of the simulations themselves short and referred to the detailed description documented elsewhere (Section 2.3). In the revised manuscript, we include more information in Section 2.3. Please refer to our detailed replies below.

The main problem, however, is that it is completely unclear which aerosol species are assessed. In subsection 2.1 of the "Methods" section (p3, l12) the authors explain they distinguish between "biomass burning" and "industrial" aerosol emissions, with substantially different single scattering albedo. This interpretation is taken up later in the discussion of results. In contrast, subsection 2.2 (p4, l7) explains that only sulfate and nitrate are investigated. In summary, after these explanations are added, and after the specific comments are addressed, I believe the paper has some merit and should be published in Geosci. Model Devel.

The anthropogenic aerosol optical properties in MACv2-SP is for all anthropogenic aerosol species. We choose a different single scattering albedo for industrially polluted regions and regions additionally affected by biomass burning for accounting for regional differences in aerosol absorption (Section 2.1). We add in Section 2.2: "Following the approach by Stevens et al. (2017), we assume that the emission of all anthropogenic aerosol species scale with the emission of SO_2 and NH_3, and therefore use these two species for scaling the anthropogenic aerosol optical depth of MACv2-SP over time. We herein use NH_3 emissions in addition to SO_2 for considering that not all dominant aerosol emission changes over time scale with the SO_2 development. (…) Aerosol absorption is represented by the single scattering albedo (Section 2.1)"

p1 l12 – it might be instructive to also report the 2090s forcing relative to 2015.

Compiling the historical evolution of the aerosol forcing is planned for RFMIP and has not yet been carried out in the framework of this study. We add in the discussion section: "RFMIP (…) will provide aerosol forcing estimates from 1850 to 2100"

p2 l10 – Mauritsen et al.: drop “and”
Dropped.

p3 l5 – “need” ! “desire”
Replaced with “desire”

p3 l27 – w is not explained. Is it some sort of weight? I don’t think it is meaningful not to specify the number of species in the sum (and in the text). Isn’t it just two?
In the revised manuscript, we move the explanation of the weights ω_k on page 4 l 5-7 to the previous paragraph: “The weight w_k describes the relative contribution of the two species, namely w_1 = 0.645 for SO2 and w_2 = 0.355 for NH3, motivated by the present-day ratio between sulphate and ammonia forcing as in Stevens et al. (2017).” and explicitly name the numbers (“k=1,2”) in the equation.

p3 l29 – p4 l1: I do not understand what the authors do here or mean. A figure might be helpful, or more text to explain.
We add a new figure for illustrating the plume centres in MACv2-SP and change here in the text: “(…) in a twenty by twenty degree box around each plume centre, marked in Figure 1.”. We further add in Section 2.1: “Figure 1 shows the annual mean of the aerosol optical depth of MACv2-SP for 2005 and the location of the nine plume centres for constructing the spatial distribution.”

p4 l4 – is that result shown somewhere, or is there a reference? - the statement needs to be corroborated or withdrawn.
We now add a figure on the comparison in the appendix and refer to it in the text: “We test the reproducibility of the regional evolution of τ_i by scaling with emissions averaged around the plume centers. For doing so, we derive E_i from a pre-existing aerosol emission database adopting the same spatial averaging, and compare the results to the corresponding E_i directly derived from the aerosol optical depth in a simulation with the aerosol-climate model ECHAM-HAM that uses the same aerosol emissions as boundary data (Figure A1). Using spatial averages of aerosol emissions around the plume centres gives E_i similar to the direct scaling from the time-evolving aerosol optical depth from the complex model. The results for E_i are herein not strongly sensitive to the choice of the number of grid boxes, e.g. a box of ten by ten degree around the plume centres only weakly modifies E_i in most cases.”

p4 l8 – the relative relevance of sulfate and nitrate depends on the abundance of SO2 and oxidants. It thus seems an oversimplification to assume it is constant with time and geographical location. Some assessment of the error introduced is at least necessary.
We show the comparison of using emission scaling and a complex aerosol-climate model for calculating the aerosol optical depth. See aloft. Here, we add: “The approach is a simplification and is meant for facilitating experimentation and a better understanding of model errors (Stevens et al., 2017).”

p4 l9 – some discussion why in particular absorbing aerosol can be neglected is necessary.
We do not neglect absorbing aerosol, but assume that the burden of absorbing aerosol scales with SO_2 and NH_3. Regional differences in absorption are represented by the single scattering albedos following Stevens et al. (2017). In addition to the details in Section 2.1., we add here: “Aerosol absorption is represented by the single scattering albedo (Section 2.1)”

p4 l12 – is this the global mean value (if so, only 0.5% difference?)? Is this similar in individual regions?

We add: "(…) global mean of (…). Regional differences are up to +/-0.039 with smaller values for 2015 in East Asia, Europe, and North America, and larger values in the other plumes".

p4 l26 – how can this affect clear-sky radiation balance?

Natural aerosols affect the radiation transfer, e.g., desert dust and sea spray. The atmospheric burden of natural aerosols is uncertain such that the clear-sky radiation balance differs amongst models. Moreover, cloud properties can be tuned. So, we generalise the statement in the revised manuscript: "to optionally tune the radiation balance of models".

p5 l8 – these are equilibrium simulations, if I understand correctly. Then "six" does not mean anything, but the length of the integration is relevant.

p5 l11 – similarly, what does "three experiments" mean in this context?

We add a new table for summarising the experiment setups and revise this section for clarifying the meaning: "For sufficiently accounting for the natural variability, we run ensembles of three simulations with the pre-industrial aerosol of 1850 and the anthropogenic aerosol from MACv2-SP. All simulations are performed for the period 2000-2010 with the same annually repeating monthly anthropogenic aerosol patterns, e.g., monthly means of the year 2005. The simulations use the same year-to-year changes of the boundary conditions, e.g., observed sea-surface temperatures. This approach is chosen for representing natural variability. The first year of each simulation is considered as the spin-up period and not used in the data analyses." and modify the paragraph on ERF: "For calculating the effective radiative forcing (ERF) of anthropogenic aerosol relative to pre-industrial, we perform experiments without τ of MACv2-SP. For this reference setup, we run an ensemble of six simulations for 2000-2010 without anthropogenic aerosol, but otherwise the same initial and boundary conditions as for the simulations with τ of MACv2-SP for efficiently increasing the number of estimates for ERF. ERF is determined as annual differences in the top of the atmosphere shortwave radiation balance from the three simulations with additionally τ from MACv2-SP and six simulations without τ from MACv2-SP. Since each simulation provides ten years for the analysis, we yield a total of 180 annual estimates of ERF for each anthropogenic aerosol pattern. "

p5 l13 – more precisely, this is decreasing the tunable parameter ntau_gl, I believe?

We decrease τ_{gl} for increasing η_N, and add in Section 2.1: "that increases η_N (Equations 3 and 4) "

p5 l14 – what motivates the name "LBG"?

LBG stands for "low background" referring to the smaller value of τ_{gl} following the name of the experiment type in Fiedler et al. (2017). We add: "low background (LBG)"

p5 l17 – what defines a specific year (i.e. why call it "2000 – 2010" rather than "2005 aerosol")? Is the sea surface temperature from observations?

Changed to: "All simulations are performed for the period 2000-2010 with the same annually repeating monthly anthropogenic aerosol patterns, e.g., monthly means of the year 2005. The simulations use the same year-to-year changes of the boundary conditions, e.g., observed sea-surface temperatures. This approach is chosen for representing natural variability. "

p5 l21 – what is “without ntau”, especially for the Twomey effect? Don’t the authors rather mean, “with scaling factor (Eq. 2) for 2090 and with scaling factor of 0”? The “180 annual estimates” make me conclude there are 6 realisations (with whatever difference between them) of 30 years integration time each. Is this correct? The authors need to explain clearly what they did.

We add a new Table 1 summarising the experiment setup and write in Section 2.3: “(…) For calculating the effective radiative forcing (ERF) of anthropogenic aerosol relative to pre-industrial, we perform experiments without τ of MACv2-SP. For this reference setup, we run an ensemble of six simulations for 2000-2010 without anthropogenic aerosol, but otherwise the same initial and boundary conditions as for the simulations with τ of MACv2-SP for efficiently increasing the number of estimates for ERF. ERF is determined as annual differences in the top of the atmosphere shortwave radiation balance from the three simulations with additionally τ from MACv2-SP and six simulations without τ from MACv2-SP. Since each simulation provides ten years for the analysis, we yield a total of 180 annual estimates of ERF for each anthropogenic aerosol pattern.” Please also refer to our reply aloft.

p5 l23 – I am lost and cannot understand why thirty. What is different between the thirty realisations?

We have 180 years of ERF and 30 years of RF for each anthropogenic aerosol pattern. Here, we have added: “Since we have three simulations for each setup with τ of MACv2-SP, we have thirty estimates of RF for each of the anthropogenic aerosol patterns.” Please also refer to our replies aloft.

p5 l25 – I strongly suggest not to overload the symbol “E” (that stands for emission scaling) but to use a different one.

We have removed the symbol and write ‘efficiency’ throughout the revised manuscript.

p6 l25 – it would be good to motivate this analysis. I would guess that there is no added information here compared to the emission scenarios. Maybe this section can be dropped.

We add the motivation: “We assess the regional characteristics in the scenarios by quantifying hemispheric differences in τ, rather than comparing mean maps of τ.”, which we have not assessed before. We perceive the analysis interesting for characterising the differences of MACv2-SP’s interpretation of the CMIP6 aerosol emission scenarios and keep this section in the manuscript.

p8 l12 – is this correlation not just by construction of the simple model?

We expect a correlation, but we prescribe the aerosol optical properties, not the forcing itself. The forcing depends on the aerosol optical properties, but also on other factors, e.g., the albedo of the underlying surface. As such, it is useful to analyse the spatial patterns and provide the figures as reference for other models that use MACv2-SP in the future.

p8 l14 – I did miss the introduction of absorption. Didn’t p4 l7 explain that only sulfate and nitrate are used?

We use the single scattering albedo for representing absorption. We add here the reference to Section 2.1 in the manuscript.

p8 l23 – a discussion on these rapid adjustments is necessary. What exactly happens here in the model?

We add: “In our model, the radiative forcing of anthropogenic aerosol from aerosol-radiation interaction and the Twomey effect induce heating perturbations. The associated change in the air temperature affects for instance the static stability of the atmosphere and thereby the circulation and embedded clouds. Such rapid adjustments cause the difference between ERF and RF, and are here summarised as net contribution.”

p12 l1 – journal is missing
We add Tellus B.

Fig. 1 – a figure showing the geographical extent of the plumes is necessary. I suggest to rather use the same scaling for all panels. A global-mean curve would be useful.
We add a new Figure 1 showing the spatial pattern of the plumes, and add in the text: “Figure 1 shows the annual mean of the aerosol optical depth of MACv2-SP for 2005 and the location of the nine plume centres for constructing the spatial distribution.”, and revised former Figure 1 (now Figure 2) for having identical axes. The global mean curves for the scenarios are shown in Figure 2 (now Figure 3).

Supplementary material: I wasn’t able to open the netcdf file. Is there a formatting mistake?
The file ending of the tar archive was removed during the handling of the uploaded file, but the netCDF files in the archive are ok.

Reviewer #2 (William Collins)

This paper provides useful documentation of the MACv2-SP aerosols that some models without their own aerosols will use for their CMIP6 simulation.

We thank you for your comments. Please note that we update the scenario names throughout the manuscript for consistency with the article by Gidden et al. (submitted).

It should be made very clear in the text that the ERFs from using these aerosols are smaller in magnitude by more than a factor of 2 than assumed by the IAMs when the scenarios were created therefore (all other factors being equal) future temperatures are likely to be less warm in these scenarios (except SSP3-ref) than expected by the IAMs, or compared to interactive aerosol models whose aerosol ERFs are closer to that of the IAMs.

We add in the conclusions: "The strength of the anthropogenic aerosol forcing has implications for the temperature development in simulations with coupled atmosphere-ocean models, e.g., a relatively weak aerosol forcing like in the standard setting of MACv2-SP likely results in a relatively stronger warming signal."

Specific comments:

Page 1, line 2: It is stated that the scenarios are based on SO2 and NH3, but elsewhere biomass burning is mentioned with different single-scattering albedo.

We choose a different single scattering albedo for industrially polluted regions and regions additionally affected by biomass burning for accounting for regional differences in aerosol absorption (Section 2.1). We add in section 2.2: "Following the approach by Stevens et al. (2017), we assume that the emission of all anthropogenic aerosol species scale with the emissions for SO_2 and NH_3, and use these two species for scaling the anthropogenic aerosol optical depth of MACv2-SP over time." In the abstract, we removed the chemical species to avoid confusion.

Page 1, line 6: "Almost all scenarios": Could mention here which one doesn't show a decrease.

Changed to: "All scenarios, except SSP3-70 and SSP4-60, show a decrease (…)"

Page 1, lines 11-13: The different SSP scenarios do not reflect an uncertainty, but rather societal choices, i.e. it is not a random outcome, but up to us to choose whether we reduce aerosols or not (there are of course uncertainties between the IAMs within each societal choice, but these aren't considered in this paper). The ERFs for the different scenarios therefore shouldn't be referred to as a spread but rather listed individually: "-0.15 for SSP1-1.9, -0.54 for SSP3-ref". To make the abstract clearer I suggest to only list ERFs, as readers can easily find the RFs in the text if they want.

We remove the values for RF and modify statements in the abstract: "We estimate the radiative forcing of anthropogenic aerosol from high- and low-end scenarios in the mid-2090s (…) The ERF of anthropogenic aerosol for the mid-2090s ranges from -0.15 Wm^{-2} for SSP1-19 to -0.54 Wm^{-2} for SSP3-70, i.e., the mid-2090s ERF is 30-108% of the value in the mid-2000s due to differences in the emission pathway alone"

Page 1, lines 13-14: Similarly the uncertainties in physics shouldn't be mixed with choices in scenario. Rather list the effects on the two extreme scenarios: "uncertainty in Twomey effect could increase these to -0.39 and -0.92.".

Changed to: "Assuming a stronger Twomey effect changes these ERFs to -0.39 Wm^{-2} and -0.92 Wm^{-2}, respectively, (…)."

Page 1: There should also be a statement of the aerosol forcings provided by the IAMs themselves (-0.365 for SSP1-1.9, -1.017 for SSP3-ref).

We add to the previous sentence: "(…) which are similar to estimates obtained from models with complex aerosol parameterisations."

Page 2, line 18: There should be some comment here or later in the text about how reasonable the linear relation between tau and emissions is.

We add the figure and description of the analysis on this topic in Section 2.2: "We test the reproducibility of the regional evolution of τ_i by scaling with emissions averaged around the plume centers. For doing so, we derive E_i from a pre-existing database adopting the same spatial averaging, and compare the results to the corresponding E_i, directly derived from the aerosol optical depth from a simulation with the aerosol-climate model ECHAM-HAM that uses the same historical aerosol emissions as boundary data (Figure A1). Using spatial averages of aerosol emissions around the plume centres gives E_i similar to the direct scaling from the time-evolving aerosol optical depth from the complex model. The results for E_i are herein not strongly sensitive to the choice of the number of grid boxes, e.g. a box of ten by ten degree around the plume centres only weakly modifies E_i in most cases."

Section 2.2: This methodology wasn't easy to follow. If the sum in eqn (2) is simply over SO2 and NH3 this should be make more explicit. Does the statement that these source "contribute one third of the total global emissions in 2005" refer to total anthopogenic+natural? If it is anthropogenic only, where do the other two thirds come from? Is the SO2/NH3 weighting the same for open burning as industrial sources – and if so why?

We revise this section, and herein use also the comments of the first reviewer. The revised manuscript has the explanation of the weights ω_k on page 4 l 5-7 in the previous paragraph: " The weight w_k describes the relative contribution of the two species, namely w_1 = 0.645 for SO2 and w_2 = 0.355 for NH3 , motivated by the present-day ratio between sulphate and ammonia forcing as in Stevens et al. (2017)." and explicitly names the numbers : "k=1,2" in the equation. We further clarify: "(…), i.e., these regions capture the dominant anthropogenic sources and contribute one third of the total global anthropogenic emissions in 2005." The SO2/NH3 weighting is the same for all plumes. We add: "The approach is a simplification and is meant for facilitating experimentation and a better understanding of model errors (Stevens et al., 2016).". Please also refer to our replies to reviewer #1 for changes in this section or the manuscript with highlighted changes for more details on the revision of this Section.

Section 2.3: This methodology wasn't easy to follow. Some tables listing all the experiments would help. It is not clear whether some of the multiples of three are identical ensembles or whether they have varying parameters (such as eta_N). How does this then lead to 180 annual estimates of ERF and thirty estimates of RF?

We add a new Table 1 for an overview on the experiments, added: "The setup of the experiments are summarised in Table 1. ", and revised Section 2.3 for clarity: Since we have three simulations for each setup with τ of MACv2-SP, we have thirty estimates of RF for each of the anthropogenic aerosol patterns. (…) For calculating the effective radiative forcing (ERF) of anthropogenic aerosol relative to pre-industrial, we perform experiments without τ of MACv2-SP. For this reference setup, we run an ensemble of six simulations for 2000-2010 without anthropogenic aerosol, but otherwise the same initial and boundary conditions as for the simulations with τ of MACv2-SP, for efficiently increasing the number of estimates for ERF. ERF is determined as annual differences in the top of the atmosphere shortwave radiation balance from the three simulations with additionally τ from MACv2-SP and six simulations without τ from MACv2-SP. Since each simulation provides ten years for the analysis, we yield a total of 180 annual estimates of ERF for each anthropogenic aerosol pattern."

Page 5, line 14: LBG should be spelled out in full, along with a short description of the implication of lowering the background.

We add: "Here, we follow the method of the low background (LBG) experiments in Fiedler et al. (2017) and set $\tau_{gl} = 0.002$ that increases η_N (Equations 3 and 4) in the experiments SSP1-26-LBG, SSP3-70-LBG, and SSP5-85-LBG of the present article."

Section 3. This needs to be clearer about which experiments are run with the 9 scenarios in table 1 and which with the 3 scenarios in table 2.

We change the introduction of Section 3.2: "We choose three scenarios for assessing the differences in the radiative forcing of anthropogenic aerosol in the mid-2090s associated with the choice of the emission pathway (Table 1). These are SSP3-70 as high-end scenario and SSP1-26 as a lower bound for the $\overline{\tau}$ spread of 0.009 to 0.027 at the end of the 21st century. The third scenario choice is SSP5-85 (…)"

Page 7, lines 31-4: The RCP scenarios used by studies cited here had very different aerosol emissions to the SSPs. Does it make sense to say your estimates are consistent?

The forcing values are similar. We change: "estimates" to "forcing values" for clarity.

Page 8, lines 8-9. It is not necessarily the variability in the rapid adjustments that causes the variability in the ERF, but rather that the methodology used is sensitive to the interannual variability in the clouds. For instance the ERF for no change in aerosols will still have a large interannual variability even though we know the rapid adjustment (and ERF) is exactly zero in every year (and indeed every timestep).

We add an explanation of the rapid adjustments in our model: "In our model, the radiative forcing of anthropogenic aerosol from aerosol-radiation interaction and the Twomey effect induce heating perturbations. The associated change in the air temperature affects for instance the static stability of the atmosphere and thereby the circulation and embedded clouds. Such rapid adjustments cause the difference between ERF and RF, and are here summarised as net contribution.". Our definition of ERF, RF and the net contribution of rapid adjustments is given in Section 2.3.

Page 8, line 12: "Efficacy" is often used for temperature response. Suggest to use "efficiency" here.

Replaced with "efficiency".

Page 8, lines 14-15: It is not obvious how the authors know the edge of the biomass burning plume is more strongly absorbing as the optical depth is only based on SO2 and NH3 emissions?

The optical properties of all anthropogenic aerosol for the mid-2000s are from the climatology MACv2 (Section 2.1), and we use SO2 and NH3 for the temporal scaling into the future (Section 2.2). We prescribe single scattering albedos for representing aerosol absorption. The single scattering albedo is smaller in biomass burning regions than in the plumes for industrial pollution, thus the absorption of the biomass burning aerosol is larger. We mark the biomass burning plumes in the new Figure 1 and add here the reference to Section 2.1 for details on the single scattering albedo.

Page 8, lines 22-24: This apparent positive rapid adjustment needs further discussion. Known adjustment processes tend to be negative (e.g. Smith et al. 2018 https://doi.org/10.1029/2018GL079826). These apparent adjustments could be the effect of circulation changes on the clouds.

Yes, we add the explanation of the "rapid adjustments in the atmosphere" of our model at the end of the paragraph. Please refer to our reply aloft for the changes in the manuscript.

Page 9, lines 7: As with the abstract these numbers should not be referred to as a spread, but as ERFs for the SSP1-1.9 and SSP3-ref scenarios.

We change these expressions throughout the manuscript. Here we change it to: “We estimate the differences in the radiative forcing of anthropogenic aerosol at the end of the 21st century that are associated with the choice of the future aerosol emission scenario (Fig. 11). For doing so, we choose three aerosol forcing scenarios that include the high- and low-end scenarios of τ in the mid-2090s. (…) MPI-ESM1.2 gives -0.15 Wm^{-2} with SSP1-26 to -0.54 Wm^{-2} with SSP3-70 for the ERF of anthropogenic aerosol for the mid-2090s (Fig. 11), reflecting the overall differences due to the anthropogenic emission pathways alone. The clear-sky forcing is herein slightly stronger with -0.24 Wm^{-2} to -0.69 Wm^{-2}, respectively, since the clouds mask radiative effects of anthropogenic aerosol.” We use ‘difference’ instead of ‘uncertainty’ in the revised Figure 11 (former Figure 10).

Page 9, lines 10-11: As before, it does not make sense to add in physical uncertainties to difference in scenario choice.

Changed to: “Assuming a stronger Twomey effect gives more negative all-sky ERFs of -0.39 Wm^{-2} to -0.92 Wm^{-2}.” We also modified Figure 11 (former Figure 10) accordingly.

Figure 1: It would be better to keep the same scale for all these.

We modified the figure for the same axes in all subfigures.

Figure 6: Use “Efficiency” rather than simply “E”.

We replace ‘E’ with ‘efficiency’ throughout the manuscript.

First forcing estimates from the future CMIP6 scenarios of anthropogenic aerosol optical properties and an associated Twomey effect

Stephanie Fiedler[1], Bjorn Stevens[1], Matthew Gidden[2], Steven J. Smith[3], Keywan Riahi[2], and Detlef van Vuuren[4,5]

[1]Max Planck Institute for Meteorology, Bundesstrasse 53, 20146, Hamburg, Germany
[2]International Institute for Applied Systems Analysis, Schlossplatz 1, A-2361 Laxenburg, Austria
[3]Joint Global Change Research Institute, Pacific Northwest National Laboratory, College Park, MD, USA
[4]Utrecht University, Vening Meineszgebouw A, Princetonlaan 8a, 3584 CB Utrecht, The Netherlands
[5]PBL Netherlands Environmental Assessment Agency, The Hague, The Netherlands

Correspondence to: Stephanie Fiedler (stephanie.fiedler@mpimet.mpg.de)

Abstract. We present the first forcing interpretation of the future anthropogenic aerosol scenarios of CMIP6 with the simple plumes parameterisation MACv2-SP. The nine scenarios for 2015 to 2100 are based on ~~SO_2 and NH_3~~ anthropogenic aerosol emissions for use in CMIP6 (Riahi et al., 2017; Gidden et al., submitted.). We use the emissions to scale the observationally informed anthropogenic aerosol optical properties and the associated effect on the cloud albedo of present-day (Fiedler et al., 2017; Stevens et al., 2017) into the future. The resulting scenarios in MACv2-SP are then ranked according to their strength in forcing magnitude and spatial asymmetries ~~. Almost all scenarios~~for anthropogenic aerosol. All scenarios, except SSP3-70 and SSP4-60, show a decrease in anthropogenic aerosol by 2100 with a range of 108% to 36% of the anthropogenic aerosol optical depth in 2015. We estimate the ~~spread in the radiative forcing associated with the~~ radiative forcing of anthropogenic aerosol from high- and low-end scenarios in the mid-2090s by performing ensembles of simulations with the atmosphere-only configuration of MPI-ESM1.2. MACv2-SP herein translates the CMIP6 emission scenarios for inducing anthropogenic aerosol forcing. With the implementation in our model, we obtain forcing estimates for both the shortwave instantaneous (RF) and effective radiative forcing (ERF) of anthropogenic aerosol relative to 1850. Here, ERF accounts for rapid atmospheric adjustments and natural variability internal to the model. The ~~spread~~ ERF of anthropogenic aerosol for the mid-2090s ~~is -0.20 to -0.57~~ranges from -0.15 Wm^{-2} ~~(-0.15~~ for SSP1-19 to -0.54 Wm^{-2} ~~) for RF (ERF) of anthropogenic aerosol, associated with uncertainty in the emission pathway alone,~~ for SSP3-70, i.e., the mid-2090s ~~forcing ranges from 33-95% (30-108%) of the~~ ERF is 30−108% of the value in the mid-2000s ~~RF (ERF). We find a larger ERF spread of -0.15 to~~ due to differences in the emission pathway alone. Assuming a stronger Twomey effect changes these ERFs to -0.39 Wm^{-2} and -0.92 Wm^{-2}, ~~when we additionally consider uncertainty in the magnitude of the Twomey effect~~respectively, which are similar to estimates obtained from models with complex aerosol parameterisations. The year-to-year standard deviations around 0.3 Wm^{-2} associated with natural variability highlights the necessity for averaging over sufficiently long time periods for estimating ERF, in contrast to RF that is typically well constrained after simulating just one year. The scenario interpretation of MACv2-SP will be used within the framework of CMIP6 and other cutting-edge scientific endeavours.

1 Introduction

Projections of future climate change require plausible assumptions on socio-economic pathways. The sixth phase of the Coupled Model Inter-comparison Project (CMIP6, Eyring et al., 2016) uses the socio-economic pathways described in O'Neill et al. (2014) and quantified by Riahi et al. (2017). Nine different emission scenarios have been defined for CMIP6 and are described in the framework of the Scenario Model Inter-comparison Project (ScenarioMIP, O'Neill et al., 2016). These emissions have been harmonised and downscaled by Gidden et al. (submitted.). The scenarios include projections of the anthropogenic aerosol emissions that we interpret here with the simple plumes parameterisation MACv2-SP (Fiedler et al., 2017; Stevens et al., 2017).

MACv2-SP parameterises radiative effects of anthropogenic aerosol, e.g., in the atmospheric component of Earth system models at the Max-Planck-Institute for Meteorology (Giorgetta et al., 2018; Müller et al., 2018; Mauritsen et al., submitted). Some MIPs endorsed by CMIP6 and other projects require the MACv2-SP parameterisation to perform the requested simulations. Such endeavours are motivated by the benefit of a consistent treatment of aerosol forcing when exploring origins of model differences in radiative forcing (RFMIP, Pincus et al., 2016) and a computationally cheap representation of aerosol effects on climate both in high-resolution simulations (HighResMIP, Haarsma et al., 2016) and in decadal climate predictions (Miklip and DCPP, Boer et al., 2016; Marotzke et al., 2016). The MACv2-SP parameterization induces aerosol-radiation interaction by prescribing anthropogenic aerosol optical properties and aerosol-cloud interaction in form of a Twomey effect by perturbing the cloud droplet number concentration. The historical development of the anthropogenic aerosol optical depth, τ, has been derived by scaling with the anthropogenic aerosol emission of the past (Stevens et al., 2017).

In the present article, we scale MACv2-SP's τ in the period 2015−2100 with the gridded CMIP6 emission scenarios of SO_2 and NH_3. The resulting scenarios in MACv2-SP are compared and classified by categories, describing the strength in forcing magnitude and spatial asymmetries. Based on the extremes in projected τ, we present the first CMIP6 ~~estimate of the spread in the~~ estimates of the radiative forcing of anthropogenic aerosol for the mid-2090s, using the atmosphere component of MPI-ESM1.2 (Mauritsen et al., submitted). The scaling method and the MPI-ESM1.2 experiments are described in Section 2, followed by the derived temporal developments of τ, the scenarios classification, and the associated ~~spread~~ difference in aerosol radiative forcing from MACv2-SP.

2 Method

2.1 MACv2-SP parameterisation

MACv2-SP is the simple plumes parameterisation for anthropogenic aerosol optical properties and an associated effect on clouds (Fiedler et al., 2017; Stevens et al., 2017). ~~It is~~ The mid-2000s values are informed by the optical properties from the aerosol climatology of the Max-Planck-Institute for Meteorology version two, MACv2, which includes additional observational data and improved regional corrections (Kinne et al., 2013; Kinne, in review). For obtaining values for the entirehistorical period, MACv2-SP uses the emission inventory endorsed by CMIP6. A detailed technical description of MACv2-SP is given by Stevens et al. (2017). Here, we focus on the description of the key characteristics and the details of the temporal scaling for the future projections.

MACv2-SP parameterises the optical properties and a relative change in the cloud droplet number concentration associated with anthropogenic aerosol as function of the geographical position, height above ground level, time, and wavelength. It is designed for the implementation in a model's radiative transfer calculation. The development of MACv2-SP was inspired by the need desire for having a computationally in-expensive and transparent representation of anthropogenic aerosol, an approach with easily changeable settings for facilitating experimentation, and a method that is flexible enough for usage in a hierarchy of model complexity and resolution.

For achieving these aims, MACv2-SP approximates the spatio-temporal distribution of τ at 550 nm from MACv2 with analytical functions. These are a superposition of two rotated Gaussian distributions at each of the nine plume centres representing regional pollution maxima, distributed across the globe. Figure 1 shows the annual mean of the aerosol optical depth of MACv2-SP for 2005 and the location of the nine plume centres for constructing the spatial distribution. We make herein a distinction between purely industrially polluted plumes and those that are additionally affected by seasonally active biomass burning. These regions differ by the level of aerosol absorption such that a different single scattering albedo is assigned, namely ω_{550nm} = 0.87 for biomass burning and ω_{550nm} = 0.93 for industrial plumes with the same asymmetry parameter of γ_{550nm} = 0.63. The vertical distributions of the aerosol extinction are approximated with beta functions, tuned to match the averaged profiles at the centre of the plumes from MACv2. Properties at wavelengths other than 550 nm are derived with an assumed Ångstrom exponent α = 2.0.

2.2 Construction of aerosol scenarios in MACv2-SP

MACv2-SP has month-to-month and year-to-year changes in τ. We adopt the same annual cycle as used for the historical reconstruction (Stevens et al., 2017). The year-to-year changes in the future scenarios are derived from the gridded aerosol emissions of anthropogenic sources and open burning specified by the CMIP6 emission scenarios (Gidden et al., submitted.). We construct time series of τ_i for each plume of the nine aerosol plume centres i using emission scaling factors, $E_i(t)$ as function of year t of the Gregorian calendar:

$$\tau_i(t) = \tau_i(2005)E_i(t), \tag{1}$$

where τ_i in 2005 is the reference valueare the reference values from the MACv2 climatology (Section 2.1). The temporal scaling, $E_i(t)$, for each of the nine aerosol scenarios in Tab. 2 are required input of the MACv2-SP parameterisation. They are available as MACv2-SP input files in netCDF format in the supplementary material. The resulting anthropogenic aerosol $\tau_i(t)$ for each scenario are presented in Section 3.1.

We construct $E_i(t)$ from the gridded CMIP6 emissions, ϵ, of the chemical species, k:

$$E_i(t) = \frac{\sum_k w_k\left[\epsilon_{ik}(t) - \epsilon_{ik}(1850)\right]}{\sum_k w_k\left[\epsilon_{ik}(2005) - \epsilon_{ik}(1850)\right]} \frac{\sum_{k=1,2} w_k\left[\epsilon_{ik}(t) - \epsilon_{ik}(1850)\right]}{\sum_{k=1,2} w_k\left[\epsilon_{ik}(2005) - \epsilon_{ik}(1850)\right]}. \tag{2}$$

~~We use~~ The weight w_k describes the relative contribution of the two species, namely $w_1 = 0.645$ for SO_2 and $w_2 = 0.355$ for NH_3, motivated by the present-day ratio between sulphate and ammonia forcing as in Stevens et al. (2017). Following the approach by Stevens et al. (2017), we assume that the emission of all anthropogenic aerosol species scale with the emission of SO_2 and NH_3, and therefore use these two species for scaling the anthropogenic aerosol optical depth of MACv2-SP over time. We herein use NH_3 emissions in addition to SO_2 for considering that not all dominant aerosol emission changes over time scale with the SO_2 development. The approach is a simplification and is meant for facilitating experimentation and a better understanding of model errors (Stevens et al., 2017). Both emissions from open burning and otherwise classified anthropogenic sources are taken into account. Aerosol absorption is represented by the single scattering albedo (Section 2.1).

We use here the gridded CMIP6 emission scenarios for the scaling, which is different from the emission scaling with ISO country codes for the historical reconstruction for MACv2-SP. For the scenarios, we average the anthropogenic emissions ϵ_{ik} in a twenty by twenty degree box around each plume centre, marked in Figure 1, where $\tau_i(2005)$ is specified and scaled over time. The spatially averaged emission flux for these nine regions exceeds the global mean by a factor of 8.5, i.e., ~~our approach captures~~ these regions capture the dominant anthropogenic sources ~~that~~ and contribute one third of the total global anthropogenic emissions in 2005.

~~We have tested~~ We test the reproducibility of the regional evolution of τ_i by scaling with emissions averaged around the plume centers. ~~Here, we derived τ_i from SO_2 emissions from~~ For doing so, we derive E_i from a pre-existing aerosol emission database adopting the same spatial averaging, and ~~compared the results against the corresponding τ_i from a transient aerosol-climate simulation of~~ compare the results to the corresponding E_i directly derived from the aerosol optical depth in a simulation with the aerosol-climate model ECHAM-HAM ~~reading the same~~ that uses the same aerosol emissions as boundary data ~~. The comparison showed that using~~ (Figure A1). Using spatial averages of ~~SO_2 already gives a good approximation of τ_i from the~~ aerosol emissions around the plume centres gives E_i similar to the direct scaling from the time-evolving aerosol optical depth from the complex model. The results for E_i are herein not strongly sensitive to the choice of the number of grid boxes, e.g. a box of ten by ten degree around the plume centres only weakly modifies E_i in most cases.

~~Here, we use NH_3 emissions in addition to SO_2 for considering that not all dominant emission changes over time scale with the SO_2 development. Both emissions from open burning and otherwise classified anthropogenic sources are taken into account. The weight w_k describes the relative contribution of the species, namely $w_{SO_2} = 0.645$ and $w_{NH_3} = 0.355$, motivated by the present-day ratio between sulphate and ammonia forcing (Stevens et al., 2017).We herein assume spatio-temporal changes of these two species as representative for all anthropogenic aerosol emissions and deliberately omit other aerosol species for consistency with the scaling approach for the historical time period (Stevens et al., 2017).~~CMIP6 specifies emissions for 2015 and every tenth year from 2020 to 2100 (Gidden et al., submitted.). We derive $E_i(t)$ at the same times and apply a linear interpolation in between. The historical reconstruction ends in 2014 and the scenarios, beginning in 2015, have a slightly larger global mean of τ by 0.0008 compared to 2014. Regional differences in the annual mean of τ are up to $+/-0.039$ with smaller values for 2015 in East Asia, Europe, and North America, and larger values in the other plumes. The values of $E_i(t)$ are all positive definite, except for the European plume in 2100 for ~~SSP4-3.4~~ SSP4-34 with a weakly negative value of -0.01. This implies a slight reduction of the total aerosol burden relative to 1850 when anthropogenic aerosol was already present in Europe associated with the industrial revolution.

The future changes in τ of the scenarios further scale MACv2-SP's magnitude of the induced Twomey effect. We mimic a Twomey effect by the pre-factor, η_N, that is parameterised as function of latitude, ϕ, and longitude, λ:

$$\eta_N(\phi,\lambda,t) = 1 + \frac{\mathrm{d}N}{N} = \frac{ln\left[1000\ \left[\tau(\phi,\lambda,t) + \tau_{\mathrm{bg}}(\phi,\lambda,t)\right] + 1\right]}{ln\left[1000\ \tau_{\mathrm{bg}}(\phi,\lambda,t) + 1\right]}. \quad (3)$$

Multiplying η_N with the cloud droplet number concentration of the host model changes the cloud optical properties with the anthropogenic aerosol perturbation. The background aerosol optical depth, τ_{bg}, is herein an idealised plume-wise approximation consistent with the setting for the historical time period (Fiedler et al., 2017; Stevens et al., 2017):

$$\tau_{\mathrm{bg}}(\phi,\lambda,t) = \tau_{\mathrm{pl}}(\phi,\lambda,t) + \tau_{\mathrm{gl}}. \quad (4)$$

The components τ_{pl} refer to a plume-shaped background and τ_{gl} to a global constant. In the standard setup of MACv2-SP, τ_{gl} is set to 0.02. This background is intended for MACv2-SP's aerosol-cloud interaction only and should not be confused with a natural aerosol pattern from observations. As emphasised by Stevens et al. (2017), this approach has been adopted so as to allow models to use their own natural aerosol for representing aerosol-radiation interaction, to optionally tune the ~~clear-sky~~ radiation balance of models, and to keep a simple formulation of the Twomey effect for adjusting the magnitude. The Twomey effect (Twomey, 1974) is qualitatively understood, but the magnitude of aerosol-cloud interactions remains uncertain (Bellouin et al., in prep.). Reasons for the difficulties to constrain the magnitude are, for instance, a shortage of suitable observations, model biases affecting radiative forcing, as well as the co-variability of meteorology and aerosol (e.g., Stevens and Feingold, 2009; Rosenfeld et al., 2014; Bony et al., 2015; Fiedler et al., 2016; Bellouin et al., in prep.). In result, different changes in N with aerosol have been proposed (Quaas et al., 2006; Andreae, 2009; Carslaw et al., 2013; Stevens et al., 2017). In the present work, we choose the original formulation by Stevens et al. (2017) for having a consistent treatment from pre-industrial to the future projections. Note that stronger aerosol-cloud interactions are also plausible (Stevens, 2015; Bellouin et al., in prep.) and can be represented by MACv2-SP, e.g., by ~~relaxing~~ reducing τ_{gl} in Eq. 4 like we do in a set of experiments here and elsewhere (Fiedler et al., 2017).

2.3 Calculation strategy for ~~spread in~~ the aerosol forcing

We perform climate simulations for estimating the anthropogenic aerosol forcing. For doing so, we use the atmosphere-only model configuration of MPI-ESM1.2 (Mauritsen et al., submitted) and follow the strategy by Fiedler et al. (2017). Natural variability internal to the model affects the effective radiative forcing estimates (Fiedler et al., 2017). For sufficiently accounting for the natural variability, we run ~~six control experiments without any anthropogenic aerosol for~~ ensembles of three simulations with the pre-industrial aerosol of 1850 and ~~six experiments with additionally prescribed~~ the anthropogenic aerosol from MACv2-SP~~for the mid-2090s.We herein~~. All simulations are performed for the period 2000−2010 with the same annually repeating monthly anthropogenic aerosol patterns, e.g., monthly means of the year 2005. The simulations use the same year-to-year changes of the boundary conditions, e.g., observed sea-surface temperatures. This approach is chosen for representing natural variability. The first year of each simulation is considered as the spin-up period and not used in the data analyses.

The setup of the experiments are summarised in Table 1. We choose three projections of τ in the mid-2090s for characterising the ~~spread in~~ difference in the anthropogenic aerosol forcing, namely the scenarios ~~SSP1-2.6, SSP3-ref, and SSP5-ref~~ SSP1-26, SSP3-70, and SSP5-85 that are introduced in Section 3.1. ~~We perform for each scenario three~~ For these scenarios, we perform experiments with the standard settings for η_N consistent with the historical reconstruction of Stevens et al. (2017). Additionally, we perform ~~another three experiments~~ experiments with increased η_N for each of these scenarios for ~~each scenario, where we increase η_N for~~ quantifying the sensitivity of the forcing ~~spread~~ differences to uncertainty in the magnitude of the Twomey effect. Here, we follow the method of the ~~LBG~~ low background (LBG) experiments in Fiedler et al. (2017) and set $\tau_{\mathrm{gl}} = 0.002$ that increases η_N (Equations 3 and 4) in the experiments ~~SSP1-2.6-LBG, SSP3-ref-LBG, and SSP5-ref-LBG~~ SSP1-26-LBG, SSP3-70-LBG, and SSP5-85-LBG of the present article. The historical forcing estimate is for the mid-2000s aerosol pattern and identical with the experiment SP in Fiedler et al. (2017).

~~All simulations are performed for the period 2000−2010 with the same annually-repeating monthly aerosol patterns for sampling natural variability with the same boundary conditions.~~

We ~~calculate the effective radiative forcing (ERF), the~~ determine the instantaneous radiative forcing (RF) ~~, and their difference as net contribution from rapid adjustments. ERF is determined as annual differences in the top of the atmosphere shortwave radiation balance with and without τ from MACv2-SP such that we yield 180 annual estimates of ERF for each mid-2090s aerosol pattern~~ of anthropogenic aerosol for the scenarios in Table 1. RF is computed online by calling the radiative transfer calculation twice, i.e., once with and once without τ of MACv2-SP. ~~We therefore have~~ Since we have three simulations for each setup with τ of MACv2-SP, we have thirty estimates of RF for each of the anthropogenic aerosol patterns. We further estimate the regional forcing ~~efficacy:~~ efficiency as:

$$E(\phi,\lambda,t) = \frac{\mathrm{RF}(\phi,\lambda,t)}{\tau(\phi,\lambda,t)} \tag{5}$$

for assessing the ~~co-variability~~ co-location of RF with τ.

~~All forcing analyses are for 2001~~

For calculating the effective radiative forcing (ERF) of anthropogenic aerosol relative to pre-industrial, we perform experiments without τ of MACv2-SP. For this reference setup, we run an ensemble of six simulations for 2000−2010 ~~, i.e., without the first year of the simulations due to the model spin-up.~~ without anthropogenic aerosol, but otherwise the same initial and boundary conditions as for the simulations with τ of MACv2-SP, for efficiently increasing the number of estimates for ERF. ERF is determined as annual differences in the top of the atmosphere shortwave radiation balance between the three simulations with additionally τ from MACv2-SP and the six simulations without τ from MACv2-SP. Since each simulation provides ten years for the analysis, we yield a total of 180 annual estimates of ERF for each anthropogenic aerosol pattern. The net contribution of rapid adjustments is the difference between ERF and RF of anthropogenic aerosol.

3 Results

3.1 Scenarios of future anthropogenic ~~AODs~~τ

3.1.1 Regionally averaged projections

The results for $\tau_i(t)$ are shown in Fig. 2 for each of the nine CMIP6 scenarios, listed in Tab. 2. Anthropogenic τ projections for East Asia are decreasing and reach levels comparable to the present-day conditions in Europe in the scenarios of SSP1, SSP2, and SSP4 by the middle of the 21st century or later. The scenarios of SSP3 and SSP5 also show decreasing τ by the end of the 21st century, but the level first increases and does not reduce as drastically as in the other SSPs. The development for Africa's anthropogenic τ is typically an increase by 2100. This projection is particularly pronounced in SSP3 and SSP4 with an increase from 2015 to 2100 by factors around two to four. The scenarios of SSP1 and SSP2 have slight τ_i increases in Africa only, whereas the scenarios of SSP5 assume an increase in Africa's τ towards the 2040s and 2080s and a subsequent decrease, respectively. Anthropogenic τ in Europe and the Americas remain comparable to the low present-day levels.

The analytical functions in MACv2-SP construct the temporally changing τ patterns from the time series of τ_i. Examples of the resulting spatial distributions of τ are shown for the mid-2050s and mid-2090s from all nine scenarios in the appendix (Fig. A2 and A3). We separate in the following MACv2-SP's scenario interpretation into differences in global mean magnitudes and spatial patterns of τ. A summary of the global mean τ and the scenario categories is provided in Tab. 2.

Magnitude differences are shown as globally averaged $\overline{\tau}$ and $\overline{\eta_N}$ in Fig. 3. ~~SSP3-ref~~ SSP3-70 stands out as the high-end scenario for both $\overline{\tau}$ and $\overline{\eta_N}$ with values exceeding the historical reconstruction for the mid-2000s and the mid-1970s. This scenario depicts socio-economic development failures associated with increasing air pollution (Riahi et al., 2017). Strong aerosol forcing is also expected from ~~SSP4-6.0 and SSP5-ref~~SSP4-60 and SSP5-85. In contrast, steep decreases in aerosol forcing are expected in SSP1, although τ reaches minima around 0.012 only after the 2030s. This scenario reflects the assumption of stringent pollution controls (Riahi et al., 2017). Towards the end of the 21st century, the ~~spread~~ difference in $\overline{\tau}$ is largest between ~~SSP3-ref~~ SSP3-70 and SSP1, with a range of 108% to 36% of the $\overline{\tau}$ in 2015 (Tab. 2). We therefore build our ~~estimate of the spread in forcing~~ estimates of the radiative forcing of anthropogenic aerosol for the mid-2090s on these scenarios (Section 3.2).

3.1.2 Spatial τ asymmetries

~~For assessing scenario differences in the spatial patterns,~~ We assess the regional characteristics in the scenarios by quantifying hemispheric differences in τ, rather than comparing mean maps of τ. For doing so, we calculate the hemispheric asymmetry from zonally averaged $\overline{\tau}$ for each latitude, ϕ:

$$A = \frac{\overline{\tau(\phi)} - \overline{\tau(-\phi)}}{2}. \quad (6)$$

In a second step, we divide A by the global mean of the same scenario, $\overline{\tau}$, for screening out magnitude differences. The results are shown for three years in Fig. 4. We find similarly large A for ~~SSP2-4.5, SSP3-ref, and SSP3-low~~ SSP2-45, SSP3-70, and

SSP3-LowNTCF that are closest to the value for 2015. For all scenarios, A is particularly large in the tropics and sub-tropics, here defined as regions equatorwards of 36° and referred to as low latitudes in the following.

All scenarios project a gradual decrease in the averaged hemispheric $\overline{A}$ in the course of the 21st century. This implies that the zonally averaged τ becomes increasingly symmetrically distributed about the equator in stark contrast to the historical reconstruction when most anthropogenic aerosol was in the northern hemisphere. We show these temporal evolutions of $\overline{A}$ and also the ratio, $\overline{A}_{\mathrm{low}\phi}/\overline{A}_{\mathrm{high}\phi}$, of the mean $\overline{A}$ in low latitudes relative to the high-latitude mean in Fig. 3. The mean $\overline{A}_{\mathrm{low}\phi}$ exceeds the value of $\overline{A}_{\mathrm{high}\phi}$ by at least a factor of two (Fig. 3), indicating that most τ is in latitudes equatorwards of 36°. ~~SSP4-3.4~~ SSP4-34 has herein by far the strongest contrast between the low and high latitudes with a factor of roughly 11 in 2100, but the overall smallest hemispheric A. This behaviour reflects the relatively symmetric τ about the equator (Fig. A3). The scenarios of SSP1 also has a stronger concentrations of anthropogenic aerosol in the low latitudes than further polewards, but a moderate hemispheric A compared to more extreme scenarios. Overall, the scenarios of SSP5 have the smallest differences between the low and high latitudes.

The scenarios in MACv2-SP are constructed with the same scaling values for the annual cycles in τ, shown in Fig. A4. Their main differences in the annual cycle of τ are associated with the variety in the spatial patterns discussed aloft. Similarities amongst the scenarios are marked (1) tropical τ maxima in the scenarios of SSP4 and ~~SSP5-ref~~ SSP5-85 for June to January, and (2) northern high-latitude τ maxima in SSP2, SSP3, and SSP5. The former maxima are herein associated with anthropogenic aerosol from biomass burning, whereas the latter is dominated by industrial emissions.

3.2 Radiative forcing of anthropogenic aerosol

3.2.1 Global means

We choose ~~SSP3-ref~~ three scenarios for assessing the differences in the radiative forcing of anthropogenic aerosol in the mid-2090s associated with the choice of the emission pathway (Table 1). These are SSP3-70 as high-end ~~scenarios and SSP1-2.6~~ scenario and SSP1-26 as a lower bound for the differences in $\overline{\tau}$ ~~spread~~ of 0.009 to 0.027 at the end of the 21st century~~for investigating the associated differences in radiative forcing. We additionally simulate SSP5-ref~~. The third scenario choice is SSP5-85 that also has a high $\overline{\tau}$ of 0.022, but interesting differences in the spatial patterns compared to ~~SSP3-ref. SSP5-ref~~ SSP3-70. SSP5-85 projects most aerosol in Africa, while ~~SSP3-ref~~ SSP3-70 most in Asia. The aerosol in Africa is seasonally dominated by biomass burning (Section 2.1), whereas aerosol in East Asia is primarily associated with industrial emissions ~~. SSP3-ref~~ (Section 2.1). SSP3-70 has herein the largest hemispheric $\overline{A}$ (Fig. 4), whereas the annual cycle in ~~SSP5-ref~~ SSP5-85 is more strongly pronounced due to the seasonally active biomass burning in Africa (Fig. A4).

Tab. 3 summarises the global mean estimates of RF and ERF. Compared to the mid-2000s, RF and ERF decrease in all scenarios, except in ~~SSP3-ref~~ SSP3-70 with the highest aerosol burden. In ~~SSP3-ref~~SSP3-70, the mid-2090s ERF of -0.54 Wm^{-2} is namely slightly stronger than for the historical estimate of -0.50 Wm^{-2} for the mid-2000s from Fiedler et al. (2017). The mid-2090s RF and ERFs are 33−95 % and 30−108 % of the mid-2000s estimates~~from Fiedler et al. (2017). This forcing spread~~. The forcing of -0.15 to -0.54 Wm^{-2} for the mid-2090s describes the ~~uncertainty~~ difference associated with the future emission pathways alone. When we ~~additionally consider the uncertainty in the~~ assume a stronger magnitude of the Twomey effect, we get ~~a larger ERF spread of -0.15~~ more negative ERFs of -0.39 $\mathrm{W m^{-2}}$ to -0.92 $\mathrm{W m^{-2}}$ (Tab. 3). Our ~~estimates~~ forcing values are consistent with earlier studies, namely the scenario ~~spread~~ difference of -0.7 to -1.0 $\mathrm{W m^{-2}}$ at the end of the 21st century from the CMIP5 configuration of HadGEM2-ES (Bellouin et al., 2011), the ACCMIP model mean estimate of -0.12 $\mathrm{W m^{-2}}$ for 2100 (Shindell et al., 2013) and the scenario ~~spread~~ difference in clear-sky RF of -0.24 to -0.37 $\mathrm{W m^{-2}}$ for 2100 from Lamarque et al. (2011).

Estimating ERF requires accounting for variability internal to the model. Fig. 6 shows the distribution of yearly estimates of ERF from the ensemble of simulations for the mid-2090s. The year-to-year standard deviations of around 0.3 $\mathrm{W m^{-2}}$ are herein comparable between the mid-2000s and all ~~the~~ our projections for the mid-2090s. This behaviour reflects that a precise estimate of ERF for any given aerosol distribution and strength requires averaging over several decades (Fiedler et al., 2017). Particularly when the ERF is small, e.g., for ~~SSP1-2.6~~SSP1-26, the year-to-year standard deviation is even larger than ERF itself (Tab. 3). Compared to ERF, the year-to-year standard deviation of RF is small, indicative of comparably stable estimates such that a one-year mean is typically sufficient for a precise estimate of a model's RF. It implies that the model-internal variability in ERF is primarily associated with the variability in the net contribution of rapid adjustments (Fig. 6).

3.2.2 Spatial patterns

The regional pattern of the clear-sky contributions to RF resembles the distribution of τ, shown in Fig. 7. Negative radiative effects herein correlate with increasing τ, shown by the similarity of the patterns in forcing ~~efficacy, E,~~ efficiency for all three scenarios of different forcing strengths. Most regions show the expected negative radiative effects associated with anthropogenic aerosol. The only exception is North Africa, where the more strongly absorbing aerosol at the edge of the biomass burning plume induces weakly positive radiative effects over the strongly reflective desert surface. In all-sky conditions, the patterns are to a great extent similar to the ones in clear-sky, but clouds mask parts of the negative radiative effects such that the regional all-sky contributions to RF are typically less negative (Fig. 8).

Including rapid adjustments strongly impairs the detectability of significant radiative effects for the mid-2090s aerosol patterns. Fig. 8 and Fig. 9 show the similarly strong impact of atmospheric variability on ERF for both high (~~SSP3-ref~~SSP3-70) and low (~~SSP1-2.6~~SSP1-26) aerosol forcing categories as well as different strengths of the Twomey effect. The impact of natural variability is consistent with findings for the patterns of the mid-1970s and mid-2000s (Fiedler et al., 2017). An interesting feature in the projection for the mid-2090s is the positive forcing in parts of central Africa. This pattern emerges primarily from rapid adjustments in the atmosphere with a relative smaller regional contribution from RF (Fig. 8). In our model, the radiative forcing of anthropogenic aerosol from aerosol-radiation interaction and the Twomey effect induce heating perturbations. The associated change in the air temperature affects for instance the static stability of the atmosphere and thereby the circulation and embedded clouds. Such rapid adjustments cause the difference between ERF and RF, and are here summarised as net contribution.

4 Conclusions

The present article presents the MACv2-SP interpretation of the future CMIP6 emissions of anthropogenic aerosol. We show the construction of the scaling parameter for the aerosol optical depth, τ, for 2015−2100 and the resulting spatio-temporal distribution of τ. The highlights of the projected aerosol developments for the 21st century are (1) a continuous stabilisation or further decrease in τ in Europe and the Americas, (2) a long-time decrease of τ in East Asia stretching over the next decades in many scenarios, and (3) steep increases in τ in Africa's biomass burning regions in most scenarios. We rank the scenarios with respect to their strengths in the aerosol forcing magnitude, the hemispheric asymmetry and the low- to high-latitude asymmetry, summarised in Fig. 10.

We estimate the ~~spread in~~ differences in the radiative forcing of anthropogenic aerosol at the end of the 21st century that ~~is associated with uncertainty in future aerosol emissions~~ are associated with the choice of the future aerosol emission scenario (Fig. 11). For doing so, we choose three aerosol forcing ~~scenario (SSP5-ref, SSP3-ref, and SSP1-2.6~~scenarios that include the high- and low-end scenarios of τ in the mid-2090s (SSP5-85, SSP3-70, and SSP1-26). Their MACv2-SP aerosol is prescribed in ensembles of simulations with the atmosphere-only configuration of MPI-ESM1.2 (Mauritsen et al., submitted), participating in CMIP6 and endorsed MIPs. The ensemble is herein useful for estimating the effective radiative forcing in light of natural variability internal to models (Fiedler et al., 2017). The year-to-year standard deviation in ERF of roughly 0.3 $\mathrm{Wm^{-2}}$ illustrates the impact of natural variability on ERF estimates that almost exclusively stems from the variability in the net contribution from rapid adjustments. Averaging over sufficiently long time periods, here 180 years, accounts for that variability. MPI-ESM1.2 gives ~~a spread of~~ -0.15 $\mathrm{Wm^{-2}}$ with SSP1-26 to -0.54 $\mathrm{Wm^{-2}}$ ~~in~~ with SSP3-70 for the ERF of anthropogenic aerosol for the mid-2090s (Fig. 11), reflecting the overall ~~uncertainty~~ differences due to the anthropogenic emission pathways alone. The clear-sky forcing is herein slightly stronger with -0.24 $\mathrm{Wm^{-2}}$ to -0.69 $\mathrm{Wm^{-2}}$, respectively, since the clouds mask radiative ~~effect~~ effects of anthropogenic aerosol. ~~Additionally considering uncertainty in the magnitude of the Twomey effect widens the spread in~~ Assuming a stronger Twomey effect gives more negative all-sky ~~ERF to -0.15 to~~ ERFs of -0.39 $\mathrm{Wm^{-2}}$ to -0.92 $\mathrm{Wm^{-2}}$ for the mid-2090s.

MACv2-SP's interpretation of the CMIP6 emission scenarios will be applied in MIPs endorsed by CMIP6 and other research activities ranging from high-resolution modelling via seasonal and decadal climate predictions to climate-change studies. The strength of the anthropogenic aerosol forcing has implications for the temperature development in simulations with coupled atmosphere-ocean models, e.g., a relatively weak aerosol forcing like in the standard setting of MACv2-SP likely results in a relatively stronger warming signal. Past studies have highlighted the role of aerosol radiative forcing for climate changes (e.g., Chung and Soden, 2017) underlining the importance of better understanding the uncertainty of anthropogenic aerosol forcing. Research initiatives such as the radiative forcing model inter-comparison project (RFMIP, Pincus et al., 2016) can help to make progress in understanding model biases causing diversity in aerosol forcing. RFMIP adopts MACv2-SP including the here-presented high-end scenario ~~SSP5-ref.~~ SSP5-85 and will provide aerosol forcing estimates from 1850 to 2100. All scenario input files for MACv2-SP are freely available in the supplementary material of this publication. We hope MACv2-

SP's scenarios will be useful for advancing our understanding of climate change and supporting impact studies for informing stakeholders.

Code and data availability. The future scaling for MACv2-SP are available in the supplementary material of this article and via input4MIPs. The code and the historical scaling of MACv2-SP is available via input4MIPs, and as supplementary material of Stevens et al. (2017). MPI-ESM1.2's code and the experiment data is stored in the tape archive of DKRZ and accessible by contacting publications@mpimet.mpg.de.

Author contributions. SF led the writing of the manuscript, constructed the scaling parameters for MACv2-SP, preformed the climate model simulations for the forcing calculations, and analysed the data. BS conceived the general concept of MACv2-SP. MG led the ScenarioMIP analysis and data generation effort and provided data for this paper. SJS led efforts to downscale scenario data to grids. KR and DvV led the coordination of ScenarioMIP. All authors contributed to the content of the manuscript.

Competing interests. The authors have no competing interests.

Acknowledgements. We would like to thank editor Andrea Stenke for handling our manuscript, as well as William Collins and an anonymous reviewer for their comments that helped improving the earlier version of this manuscript. We acknowledge the use of the data from the CMIP6 emission scenarios and the supercomputer facilities of the DKRZ. SF and BS thank the Max-Planck-Society for funding this work.

References

Andreae, M. O.: Correlation between cloud condensation nuclei concentration and aerosol optical thickness in remote and polluted regions, Atmospheric Chemistry and Physics, 9, 543–556, doi:10.5194/acp-9-543-2009, 2009.

Bellouin, N., Rae, J., Jones, A., Johnson, C., Haywood, J., and Boucher, O.: Aerosol forcing in the Climate Model Intercomparison Project (CMIP5) simulations by HadGEM2-ES and the role of ammonium nitrate, J. Geophys. Res, 116, D20 206, doi:10.1029/2011JD016074, 2011.

Bellouin, N., Daniau, A.-L., Feingold, G., Fiedler, S., Gettleman, A., Gryspeerdt, E., Haywood, J., Lohmann, U., ~~M.~~ Mülmenstädt, J., Possner, A., Quaas, J., Storelvmo, T., Toll, V., Watson-Parris, D., and et al.: Bounding aerosol radiative forcing, in prep.

Boer, G. J., Smith, D. M., Cassou, C., Doblas-Reyes, F., Danabasoglu, G., Kirtman, B., Kushnir, Y., Kimoto, M., Meehl, G. A., Msadek, R., Mueller, W. A., Taylor, K. E., Zwiers, F., Rixen, M., Ruprich-Robert, Y., and Eade, R.: The Decadal Climate Prediction Project (DCPP) contribution to CMIP6, Geoscientific Model Development, 9, 3751–3777, doi:10.5194/gmd-9-3751-2016, 2016.

Bony, S., Stevens, B., Frierson, D. M., Jakob, C., Kageyama, M., Pincus, R., Shepherd, T. G., Sherwood, S. C., Siebesma, A. P., Sobel, A. H., et al.: Clouds, circulation and climate sensitivity, Nature Geoscience, 8, 261–268, doi:10.1038/ngeo2398, 2015.

Carslaw, K., Lee, L., Reddington, C., Pringle, K., Rap, A., Forster, P., Mann, G., Spracklen, D., Woodhouse, M., Regayre, L., et al.: Large contribution of natural aerosols to uncertainty in indirect forcing, Nature, 503, 67–71, 2013.

Chung, E.-S. and Soden, B. J.: Hemispheric climate shifts driven by anthropogenic aerosol–cloud interactions, Nature Geoscience, 10, 566, 2017.

Eyring, V., Bony, S., Meehl, G. A., Senior, C. A., Stevens, B., Stouffer, R. J., and Taylor, K. E.: Overview of the Coupled Model Intercomparison Project Phase 6 (CMIP6) experimental design and organization, Geosci. Model Dev., 9, 1937–1958, doi:10.5194/gmd-9-1937-2016, 2016.

Fiedler, S., Knippertz, P., Woodward, S., Martin, G. M., Bellouin, N., Ross, A. N., Heinold, B., Schepanski, K., Birch, C. E., and Tegen, I.: A process-based evaluation of dust-emitting winds in the CMIP5 simulation of HadGEM2-ES, Climate Dynamics, 46, 1107–1130, doi:10.1007/s00382-015-2635-9, 2016.

Fiedler, S., Stevens, B., and Mauritsen, T.: On the sensitivity of anthropogenic aerosol forcing to model-internal variability and parameterizing a Twomey effect, J. Adv. Model. Earth Syst., pp. n/a–n/a, doi:10.1002/2017MS000932, 2017.

Gidden, M. J., Riahi, K., ~~van~~ Smith, S. J., Fujimori, S., Luderer, G., Kriegler, E., van Vuuren, D. P., van den Berg, M., Feng, L., Klein, D., ~~Fujimori, S., Feng, L.,~~ Calvin, K., Doelman, J., Frank, S., Fricko, O., ~~Horing, J., Luderer, G., Kriegler, E., Smith, S.~~ Harmsen, M., Hasegawa, T., Havlik, P., Hilaire, J., Hoesly, R., Horing, J., ~~and van Vuuren, D~~Popp, A., Stehfest, E., and Takahashi, K.: Global emissions pathways under different socioeconomic scenarios for use in CMIP6: a dataset of harmonized regional and country-level emissions trajectories through the end of the century, Geosci. Model Dev., ~~in prep~~submitted.

Giorgetta, M. A., Brokopf, R., Crueger, T., Esch, M., Fiedler, S., Helmert, J., Hohenegger, C., Kornblueh, L., Köhler, M., Manzini, E., Mauritsen, T., Nam, C., Raddatz, T., Rast, S., Reinert, D., Sakradzija, M., Schmidt, H., Schneck, R., Schnur, R., Silvers, L., Wan, H., Zängl, G., and Stevens, B.: ICON-A, the Atmosphere Component of the ICON Earth System Model: I. Model Description, Journal of Advances in Modeling Earth Systems, 10, 1613–1637, doi:10.1029/2017MS001242, 2018.

Haarsma, R. J., Roberts, M. J., Vidale, P. L., Senior, C. A., Bellucci, A., Bao, Q., Chang, P., Corti, S., Fučkar, N. S., Guemas, V., von Hardenberg, J., Hazeleger, W., Kodama, C., Koenigk, T., Leung, L. R., Lu, J., Luo, J.-J., Mao, J., Mizielinski, M. S., Mizuta, R., Nobre, P., Satoh, M., Scoccimarro, E., Semmler, T., Small, J., and von Storch, J.-S.: High Resolution Model Intercomparison Project (HighResMIP v1.0) for CMIP6, Geoscientific Model Development, 9, 4185–4208, doi:10.5194/gmd-9-4185-2016, https://www.geosci-model-dev.net/9/4185/2016/, 2016.

Kinne, S.: The Max-Planck Aerosol Climatology, version 2, ~~submitted~~Tellus B, in review.

Kinne, S., O'Donnel, D., Stier, P., Kloster, S., Zhang, K., Schmidt, H., Rast, S., Giorgetta, M., Eck, T. F., and Stevens, B.: MAC-v1: A new global aerosol climatology for climate studies, Journal of Advances in Modeling Earth Systems, 5, 704–740, doi:10.1002/jame.20035, 2013.

Lamarque, J.-F., Kyle, G. P., Meinshausen, M., Riahi, K., Smith, S. J., van Vuuren, D. P., Conley, A. J., and Vitt, F.: Global and regional evolution of short-lived radiatively-active gases and aerosols in the Representative Concentration Pathways, Climatic Change, 109, 191, https://doi.org/10.1007/s10584-011-0155-0, 2011.

Marotzke, J., Müller, W. A., Vamborg, F. S. E., Becker, P., Cubasch, U., Feldmann, H., Kaspar, F., Kottmeier, C., Marini, C., Polkova, I., Prömmel, K., Rust, H. W., Stammer, D., Ulbrich, U., Kadow, C., Köhl, A., Kröger, J., Kruschke, T., Pinto, J. G., Pohlmann, H., Reyers, M., Schröder, M., Sienz, F., Timmreck, C., and Ziese, M.: MiKlip: A National Research Project on Decadal Climate Prediction, Bulletin of the American Meteorological Society, 97, 2379–2394, doi:10.1175/BAMS-D-15-00184.1, 2016.

Mauritsen, T.~~and~~ , et al.: Developments in the MPI-M Earth System Model version 1.2 (MPI-ESM1.2) and its response to increasing CO2, submitted.

Müller, W. A., Jungclaus, J. H., Mauritsen, T., Baehr, J., Bittner, M., Budich, R., Bunzel, F., Esch, M., Ghosh, R., Haak, H., Ilyina, T., Kleine, T., Kornblueh, L., Li, H., Modali, K., Notz, D., Pohlmann, H., Roeckner, E., Stemmler, I., Tian, F., and Marotzke, J.: A Higher-resolution Version of the Max Planck Institute Earth System Model (MPI-ESM1.2-HR), Journal of Advances in Modeling Earth Systems, 10, 1383–1413, doi:10.1029/2017MS001217, 2018.

O'Neill, B. C., Tebaldi, C., van Vuuren, D. P., Eyring, V., Friedlingstein, P., Hurtt, G., Knutti, R., Kriegler, E., Lamarque, J.-F., Lowe, J., Meehl, G. A., Moss, R., Riahi, K., and Sanderson, B. M.: The Scenario Model Intercomparison Project (ScenarioMIP) for CMIP6, Geoscientific Model Development, 9, 3461–3482, doi:10.5194/gmd-9-3461-2016, 2016.

~~O?~~

O'Neill, B. C., Kriegler, E., Riahi, K., Ebi, K. L., Hallegatte, S., Carter, T. R., Mathur, R., and van Vuuren, D. P.: A new scenario framework for climate change research: the concept of shared socioeconomic pathways, Climatic Change, 122, 387–400, 2014.

Pincus, R., Forster, P. M., and Stevens, B.: The Radiative Forcing Model Intercomparison Project (RFMIP): experimental protocol for CMIP6, Geoscientific Model Development, 9, 3447–3460, doi:10.5194/gmd-9-3447-2016, 2016.

Quaas, J., Boucher, O., and Lohmann, U.: Constraining the total aerosol indirect effect in the LMDZ and ECHAM4 GCMs using MODIS satellite data, Atmospheric Chemistry and Physics, 6, 947–955, doi:10.5194/acp-6-947-2006, http://www.atmos-chem-phys.net/6/947/2006/, 2006.

Riahi, K., van Vuuren, D. P., Kriegler, E., Edmonds, J., O'Neill, B. C., Fujimori, S., Bauer, N., Calvin, K., Dellink, R., Fricko, O., Lutz, W., Popp, A., Cuaresma, J. C., KC, S., Leimbach, M., Jiang, L., Kram, T., Rao, S., Emmerling, J., Ebi, K., Hasegawa, T., Havlik, P., Humpenöder, F., Silva, L. A. D., Smith, S., Stehfest, E., Bosetti, V., Eom, J., Gernaat, D., Masui, T., Rogelj, J., Strefler, J., Drouet, L., Krey, V., Luderer, G., Harmsen, M., Takahashi, K., Baumstark, L., Doelman, J. C., Kainuma, M., Klimont, Z., Marangoni, G., Lotze-Campen, H., Obersteiner, M., Tabeau, A., and Tavoni, M.: The Shared Socioeconomic Pathways and their energy, land use, and greenhouse gas emissions implications: An overview, Global Environmental Change, 42, 153 – 168, doi:10.1016/j.gloenvcha.2016.05.009, 2017.

Rosenfeld, D., Sherwood, S., Wood, R., and Donner, L.: Climate Effects of Aerosol-Cloud Interactions, Science, 343, 379–380, doi:10.1126/science.1247490, 2014.

Shindell, D. T., Lamarque, J.-F., Schulz, M., Flanner, M., Jiao, C., Chin, M., Young, P. J., Lee, Y. H., Rotstayn, L., Mahowald, N., Milly, G., Faluvegi, G., Balkanski, Y., Collins, W. J., Conley, A. J., Dalsoren, S., Easter, R., Ghan, S., Horowitz, L., Liu, X., Myhre, G., Nagashima, T., Naik, V., Rumbold, S. T., Skeie, R., Sudo, K., Szopa, S., Takemura, T., Voulgarakis, A., Yoon, J.-H., and Lo, F.: Radiative forcing in the ACCMIP historical and future climate simulations, Atmospheric Chemistry and Physics, 13, 2939–2974, doi:10.5194/acp-13-2939-2013, 2013.

Stevens, B.: Rethinking the lower bound on aerosol radiative forcing, Journal of Climate, 28, 4794–4819, doi:10.1175/JCLI-D-14-00656.1, 2015.

Stevens, B. and Feingold, G.: Untangling aerosol effects on clouds and precipitation in a buffered system, Nature, 461, 607–613, 2009.

Stevens, B., Fiedler, S., Kinne, S., Peters, K., Rast, S., Müsse, J., Smith, S. J., and Mauritsen, T.: MACv2-SP: a parameterization of anthropogenic aerosol optical properties and an associated Twomey effect for use in CMIP6, Geosci. Mod. Dev., 10, 433–452, doi:10.5194/gmd-10-433-2017, 2017.

Twomey, S.: Pollution and the planetary albedo, Atmos. Environ., 8, 1251–1256, 1974.

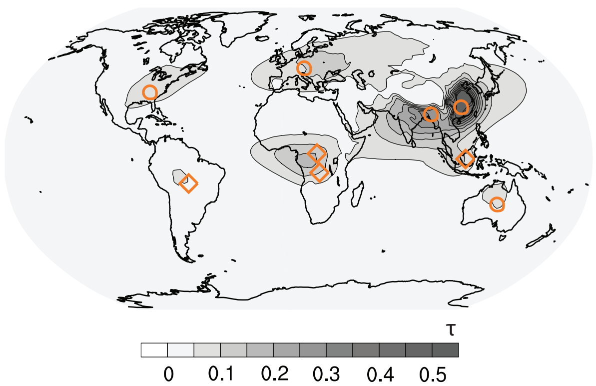

Figure 1. Aerosol optical depth of MACv2-SP for 2005. Locations of the nine aerosol plume centres are marked in orange with circles for industrial pollution and rectangles for seasonally active biomass burning.

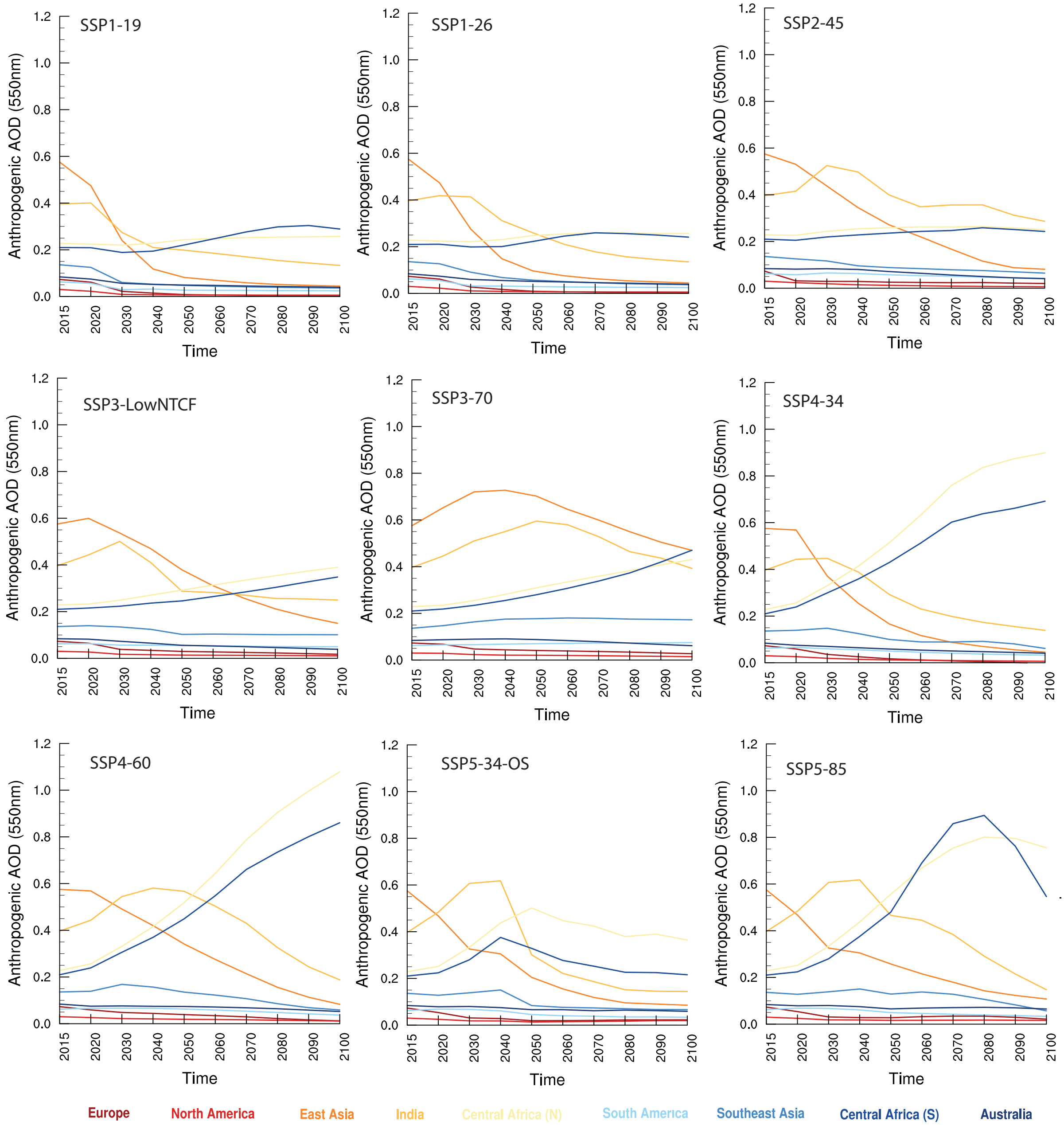

Figure 2. Future τ_i in the MACv2-SP interpretation of CMIP6 scenarios. Shown are the temporal developments of anthropogenic aerosol optical depth, τ, at 550 nm in the colour-coded aerosol plumes of MACv2-SP for the nine emission scenarios of CMIP6. Note the different scales.

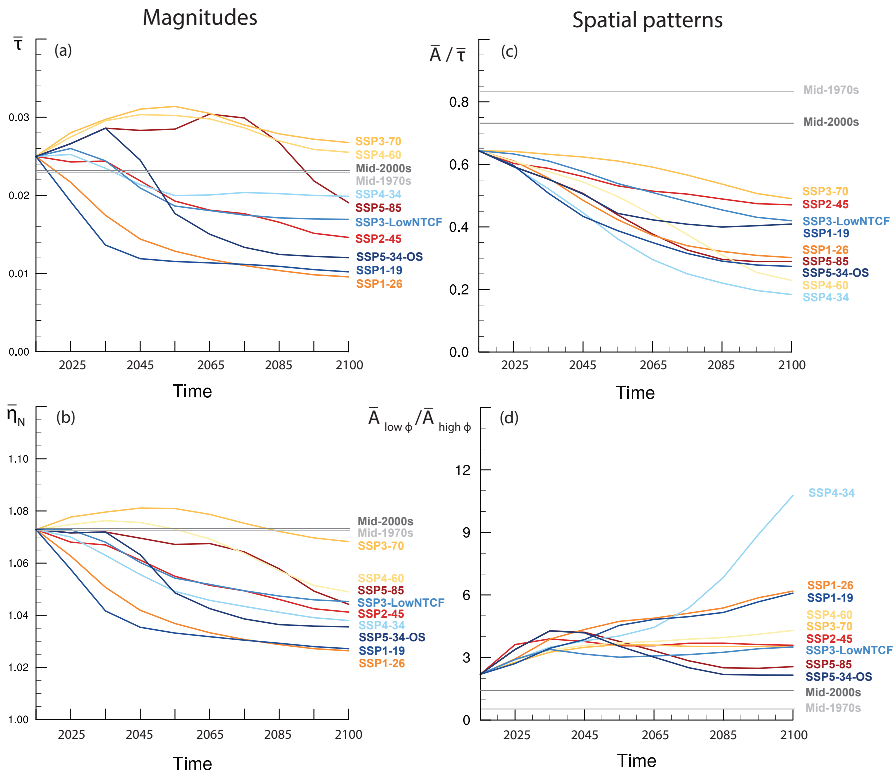

Figure 3. Future developments of global means in the MACv2-SP interpretation of CMIP6 scenarios. Shown are the temporal developments of annual averages in (a) $\overline{\tau}$ at 550 nm for inducing aerosol-radiation interaction and (b) $\overline{\eta_N}$ for mimicking aerosol-cloud interaction, as well as (c) hemispheric asymmetry in τ, $\overline{A}$, weighted by the global mean $\overline{\tau}$ and (d) ratio of A in low latitudes ($\phi < 36°$) relative to higher latitudes. MACv2-SP's ranking of the emission scenarios of CMIP6 for their strength in (left) the forcing magnitude and (right) spatial asymmetry is shown with the colour-coded labels on the right. Reference values of the mid-1970s and mid-2000s from the historical reconstruction (Fiedler et al., 2017; Stevens et al., 2017) are indicated by grey lines.

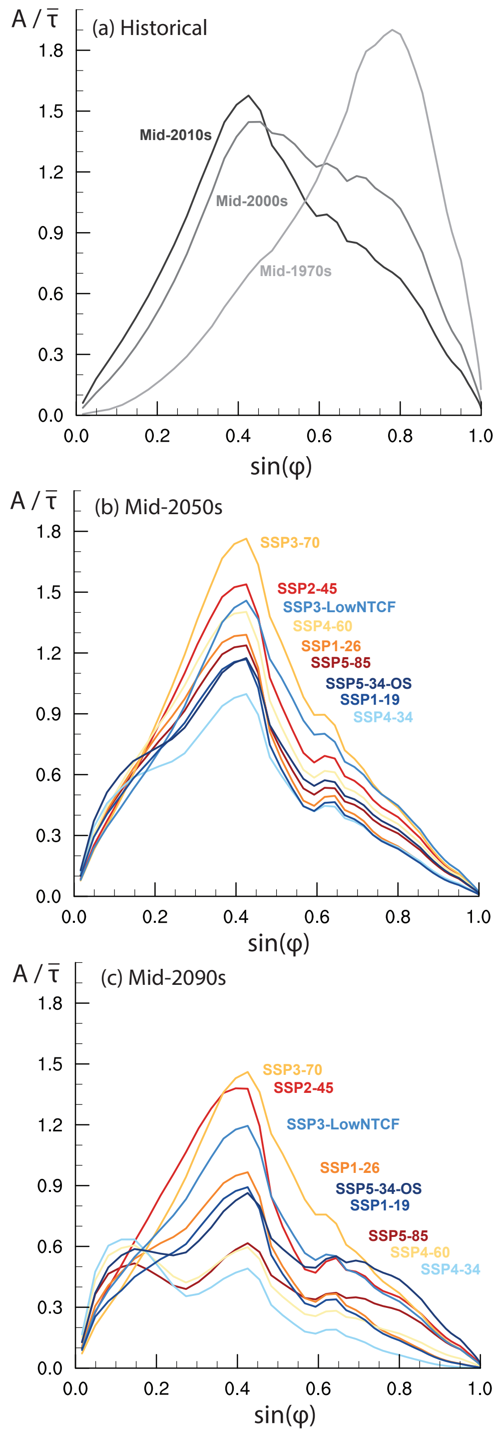

Figure 4. Hemispheric asymmetry of τ in the MACv2-SP interpretation of CMIP6 scenarios. Shown are the hemispheric asymmetry, A, weighted by the the global mean τ. All values are computed for τ at 550 nm for (a) selected years from the historical reconstruction, as well as each CMIP6 emission scenario for both (b) the mid-2050s and (c) mid-2090s.

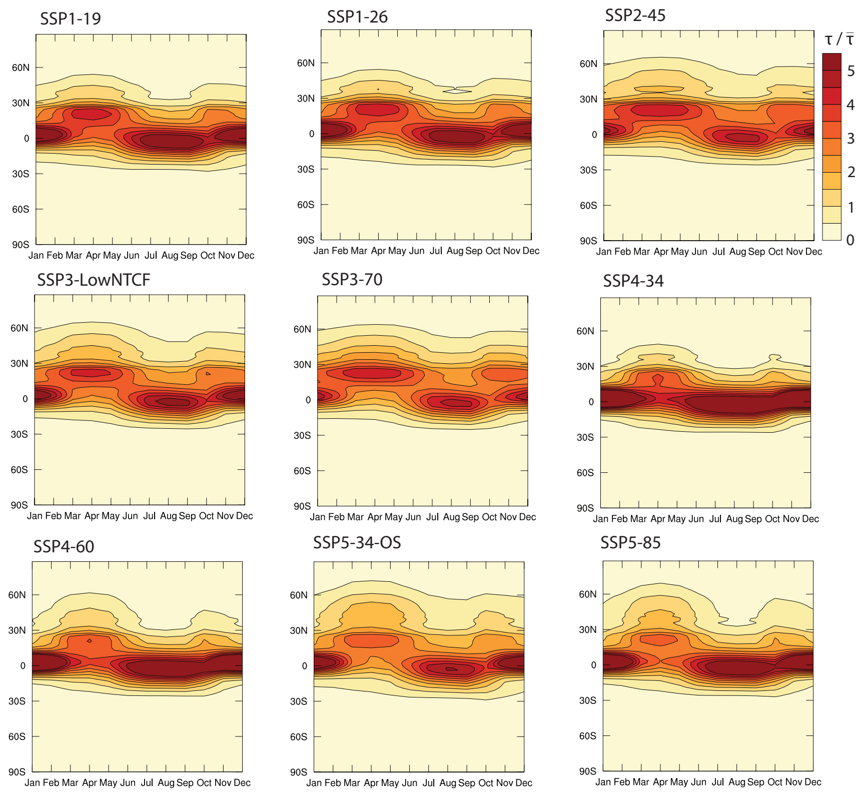

Figure 5. Spatial patterns for the mid-2090s in the MACv2-SP interpretation of CMIP6 scenarios. Shown are the annual cycles of the zonal means in τ at 550 nm weighted by the global mean $\overline{\tau}$ for each month and emission scenario of CMIP6.

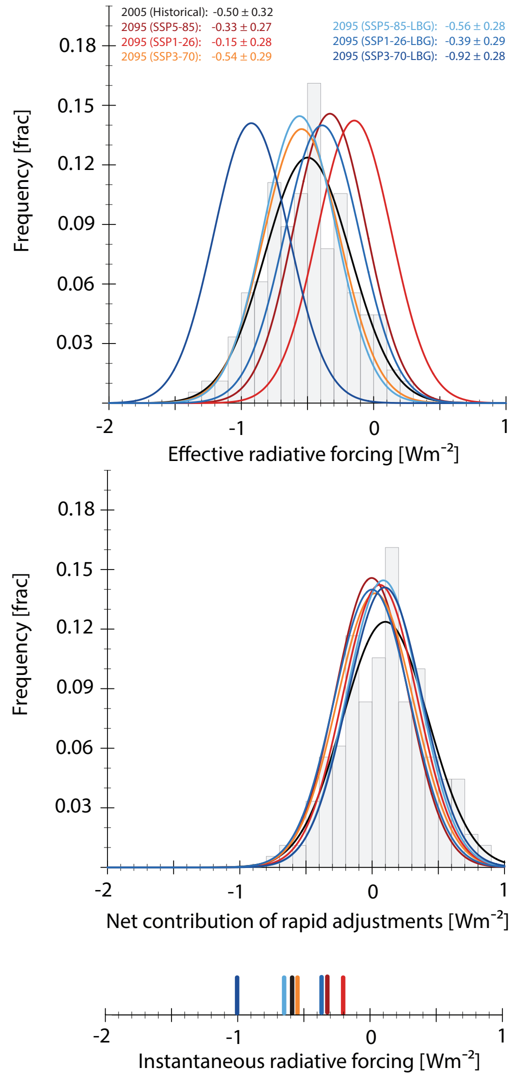

Figure 6. Natural variability in all-sky forcing for the mid-2090s. Shown are the Gaussian distributions of (top) the effective radiative forcing (ERF) and (middle) the net contribution of rapid adjustments for the mid-2090s with (orange-red) the standard and (blue) the stronger Twomey effects. The black line marks the mid-2000s values from Fiedler et al. (2017) with the frequency histogram in grey. The distributions are based on annual means for all-sky condition in the shortwave spectrum (SW) at the top of the atmosphere (TOA). The long-term means +/- year-to-year standard deviation of annual ERFs are listed at the top. The year-to-year standard deviation herein illustrate the impact of natural variability internal to the model on estimating ERF, in contrast to the (bottom) annual means in the instantaneous radiative forcing (RF) that are not strongly affected by natural variability.

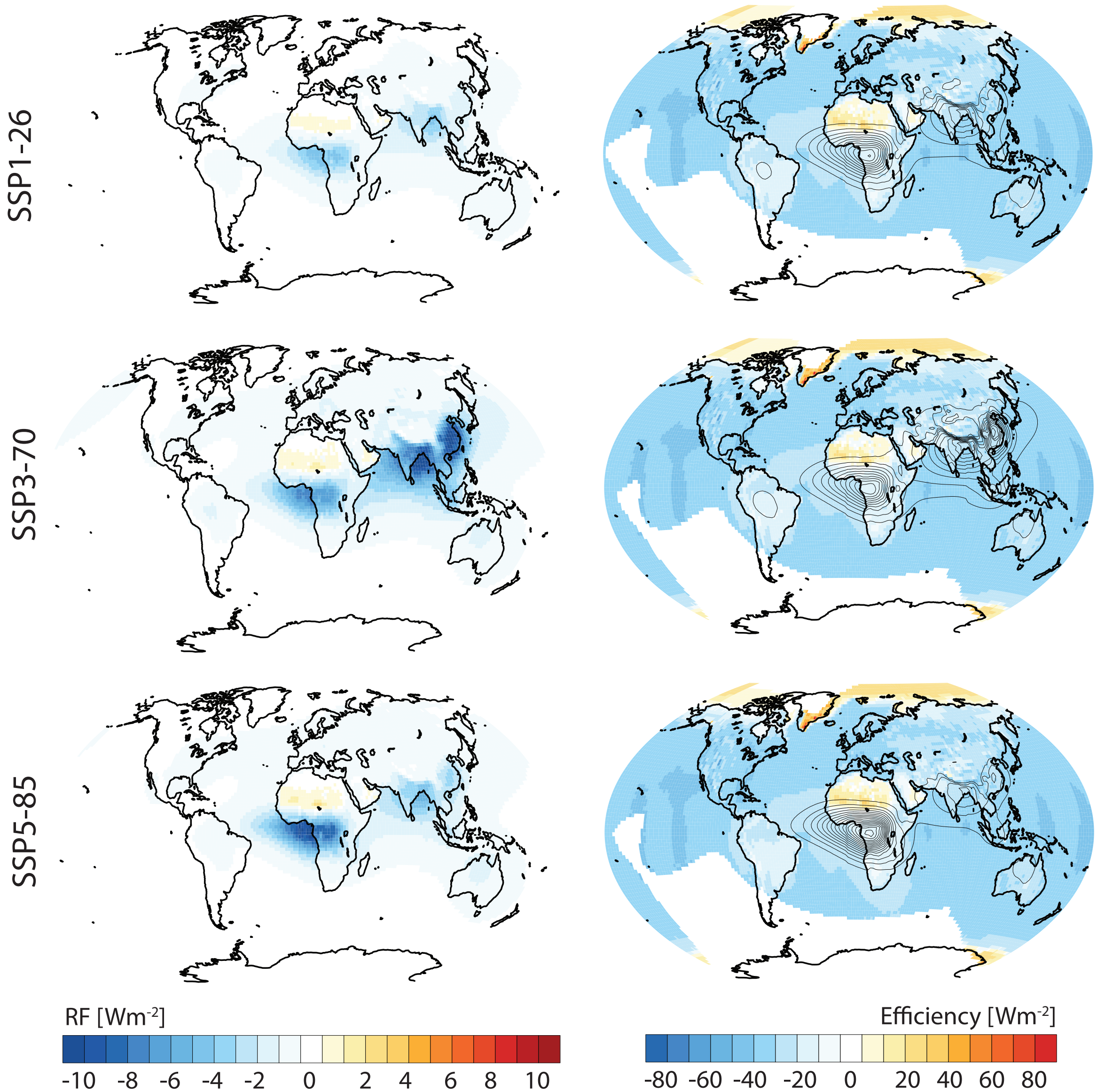

Figure 7. Clear-sky RF and E for the mid-2090s. Shown are the (left) SW TOA instantaneous radiative forcing and (right) forcing ~~efficacy, E,~~ efficiency as RF devided by ~~the anthropogenic aerosol optical depth,~~ τ. Contours show τ at 550 nm from 0.04 in steps of 0.04 (compare Fig. A3). All forcings are for clear-sky conditions in mid-2090s from selected CMIP6 emission scenarios.

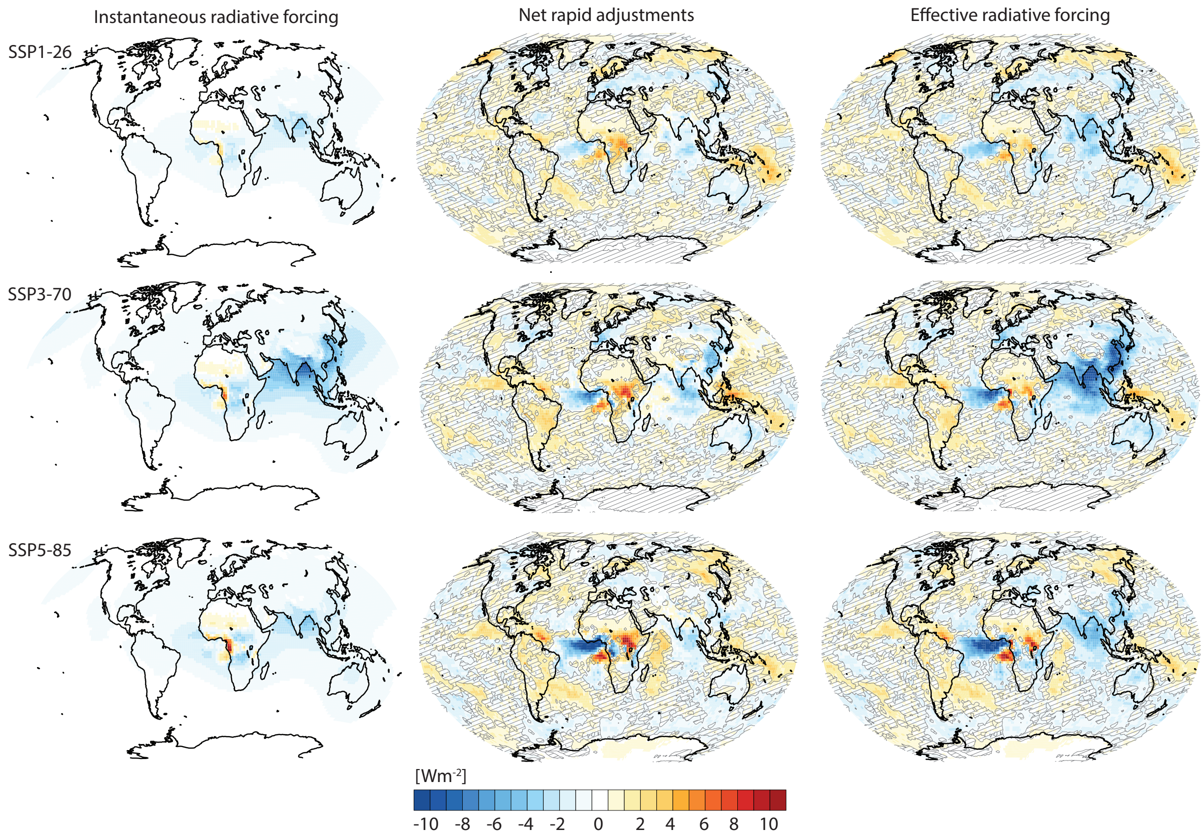

Figure 8. All-sky radiative forcing for the mid-2090s. Shown are the SW TOA (left) RF, (middle) the net contribution from rapid adjustments, and (right) ERF for all-sky conditions in the mid-2090s from the CMIP6 emission scenarios. ERFs not significantly different from zero are masked out by hatching, adopting a confidence level of 10%.

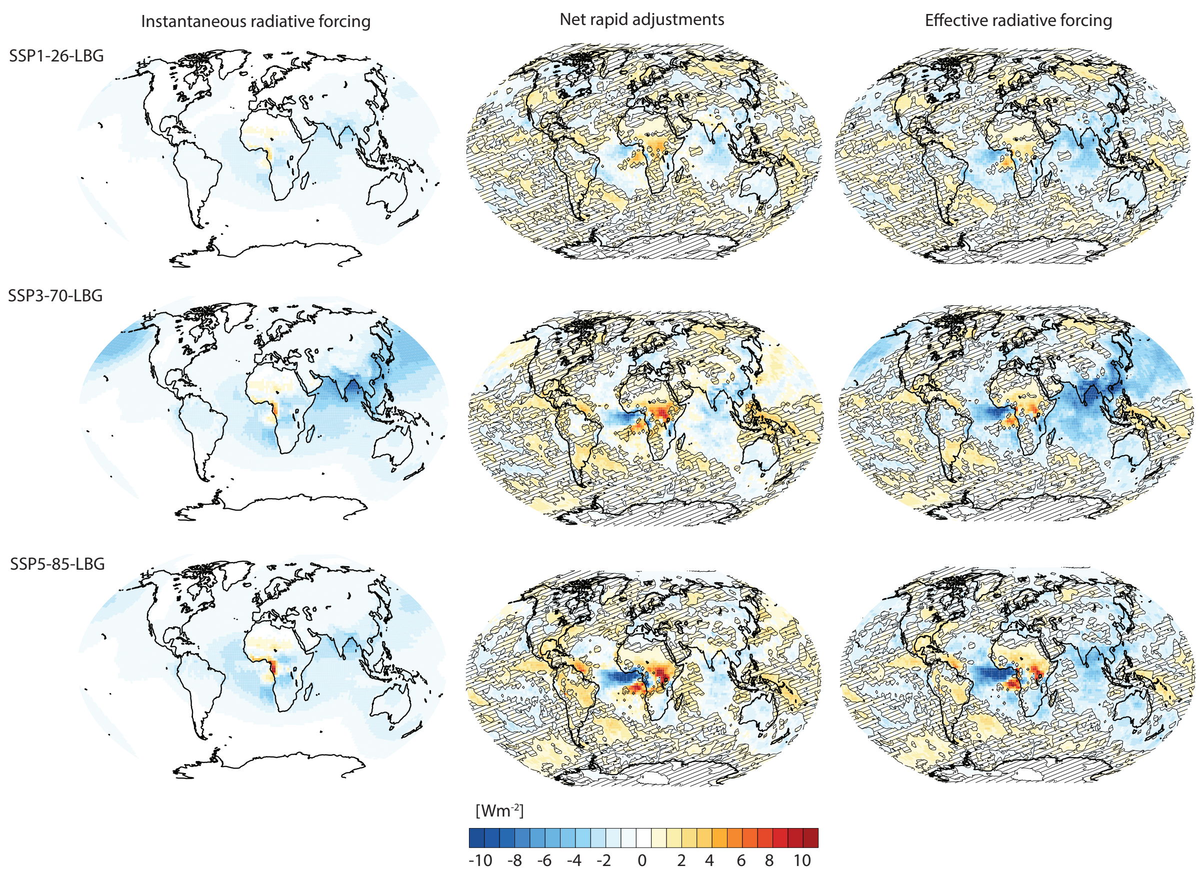

Figure 9. All-sky radiative forcing for the mid-2090s with strong Twomey effects. As Fig. 8, but with stronger Twomey effects by increasing η_N (Section 2).

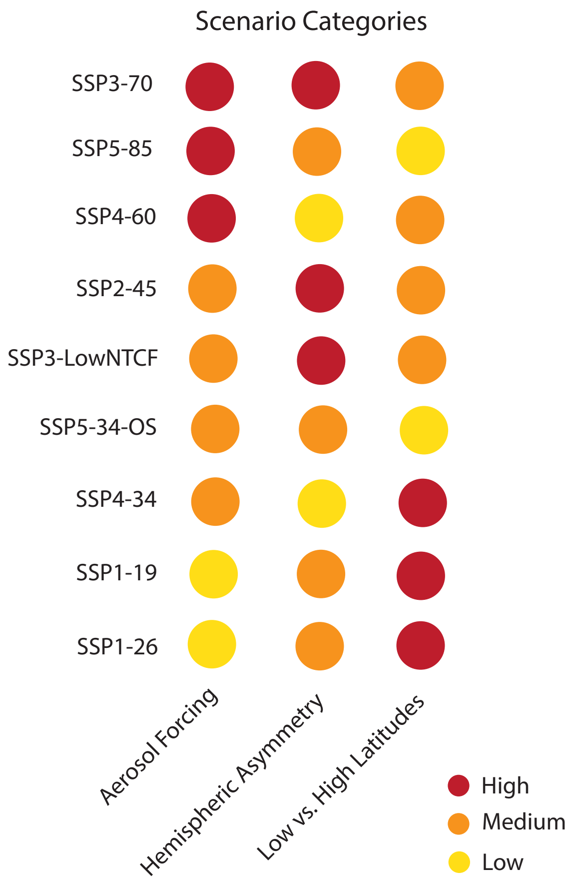

Figure 10. Categories in the MACv2-SP interpretation of the CMIP6 anthropogenic aerosol scenarios. Shown is the colour-coded ranking of the CMIP6 scenarios with respect to the strength in the aerosol forcing, the hemispheric asymmetry, and the low- to high-latitude difference in the asymmetry.

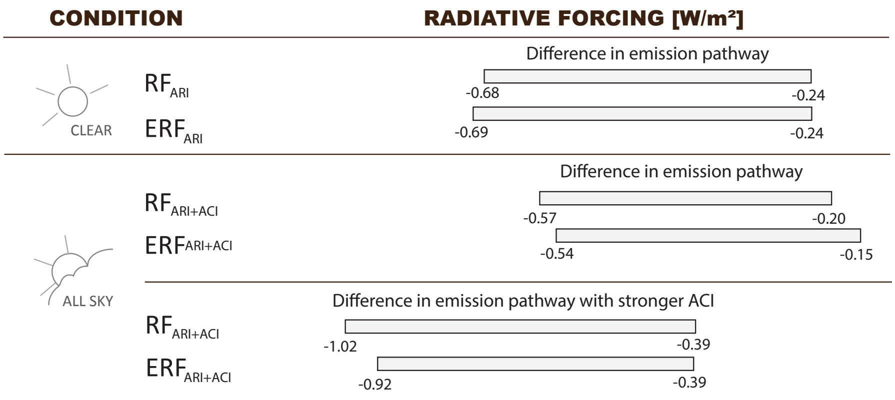

Figure 11. Spread Difference in anthropogenic aerosol radiative forcing of the MACv2-SP interpretation of the CMIP6 scenarios for the mid-2090s. Summarised are the instantaneous (RF) and effective radiative forcing (ERF) from aerosol-radiation interaction (ARI) and aerosol-cloud interaction (ACI), based on the high-end scenarios SSP3-refSSP3-70, SSP5-refSSP5-85, and SSP1-2.6 SSP1-26 as low-emission scenario for the upper bound. The spread is bars illustrate the difference in forcing uncertainty associated with the emission pathways of CMIP6.Additionally, we show the spread when uncertainties in both the emission pathway and the magnitude of the Twomey effect are considered.

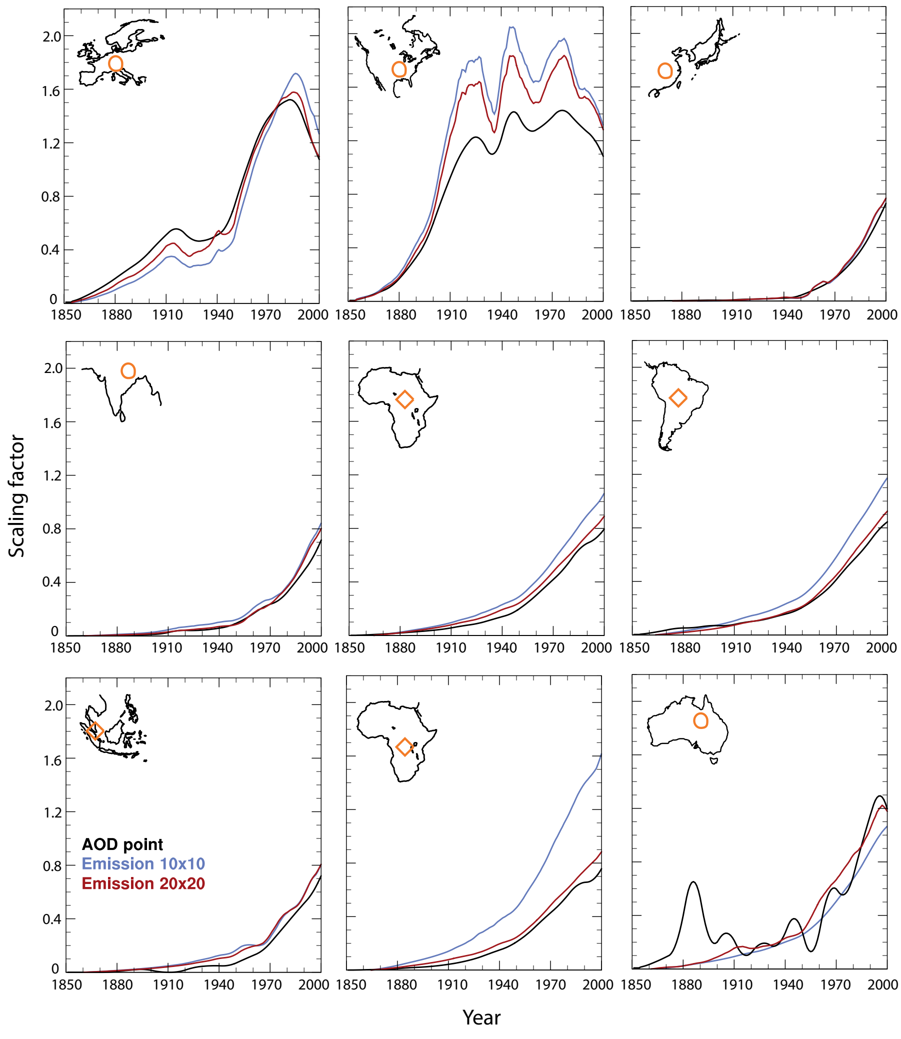

Figure A1. Scaling factor comparison. Shown are annual scaling factors $E_i(t)$ derived from (black) the aerosol optical depth in the plume centres of a transient ECHAM-HAM simulation, and (colours) the anthropogenic aerosol emissions of that simulation, averaged over grid boxes around the plume centres. The geographical positions of the plumes with (circles) industrial pollution and (rectangles) biomass burning are indicated.

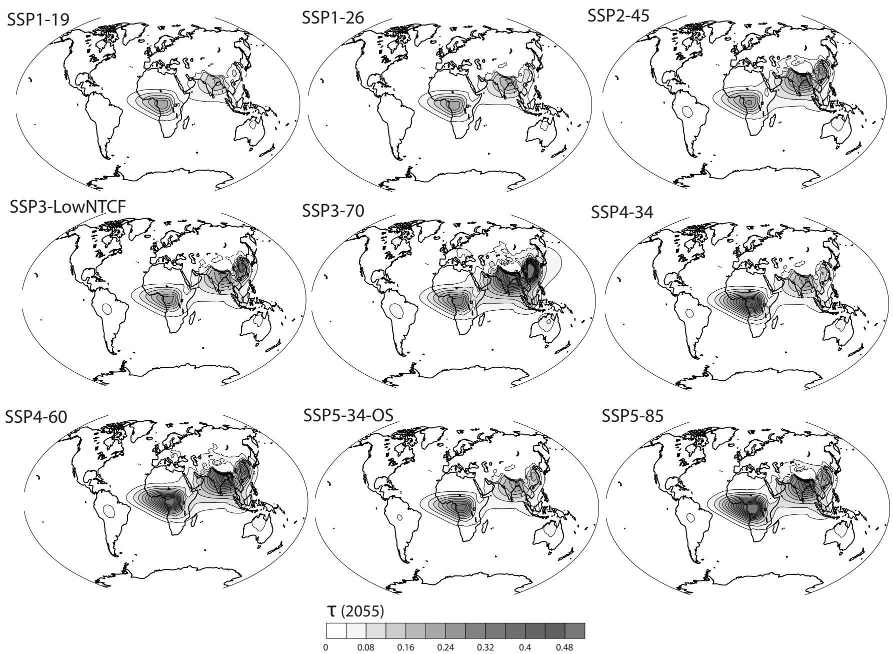

Figure A2. τ scenarios for the mid-2050s in MACv2-SP. Shown are the spatial distributions of τ at 550 nm in the mid-2050s for each of the nine emission scenarios of CMIP6.

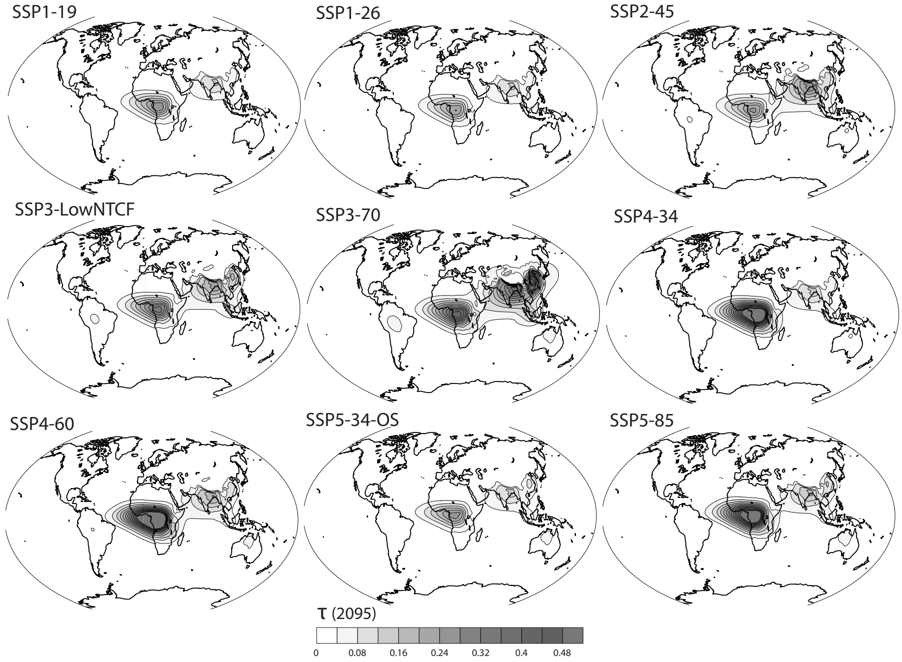

Figure A3. τ scenarios for the mid-2090s in MACv2-SP. As Fig. A2, but projection for the mid-2090s.

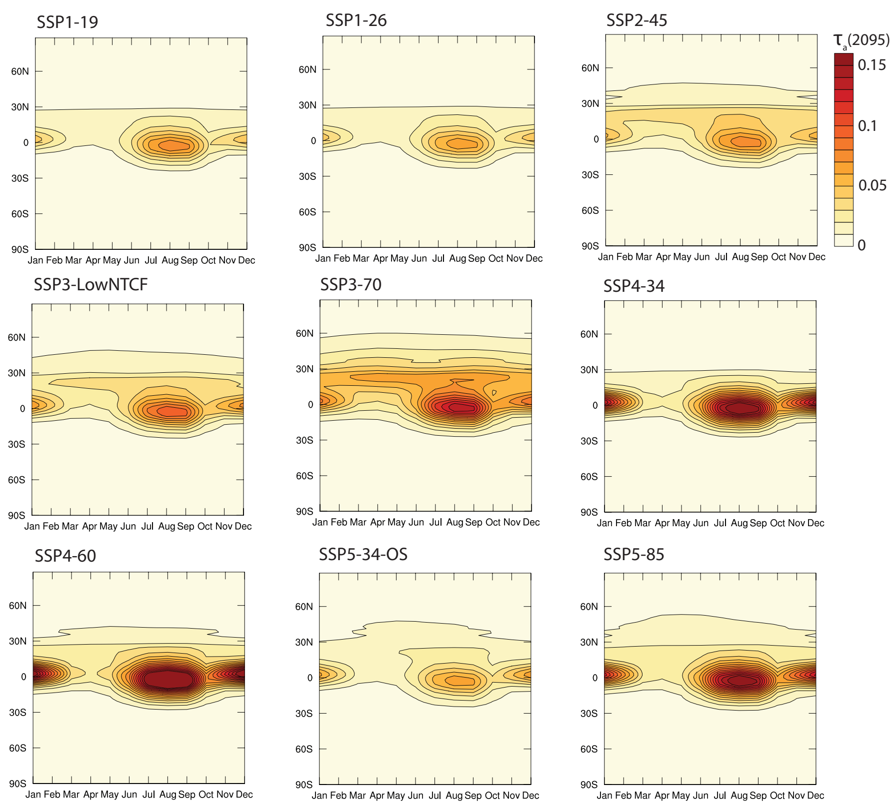

Figure A4. τ scenarios for the mid-2090s in MACv2-SP. Shown are the annual cycles of the zonal means in τ at 550 nm in the mid-2090s for each of the nine emission scenarios of CMIP6.

Table 1. Experiment setup for estimating forcing.

Experiment name	Natural aerosol	Anthropogenic aerosol	Twomey effect	No. of ten-year simulations
Reference	1850	none	none	6
mid-2000s	1850	mid-2000s	standard ($\tau_{gl} = 0.02$)	3
SSP1-26				
SSP3-70	1850	mid-2090s	standard ($\tau_{gl} = 0.02$)	3
SSP5-85				
SSP1-26-LBG				
SSP3-70-LBG	1850	mid-2090s	strong ($\tau_{gl} = 0.002$)	3
SSP5-85-LBG				

Table 2. Anthropogenic aerosol scenarios for MACv2-SP ($\overline{\tau}$=0.025 in 2015).

Scenario ~~name~~ Name	Mean $\overline{\tau}$ (2050s)	Mean $\overline{\tau}$ (2090s)	Aerosol Forcing category	Hemispheric Asymmetry category	Low vs. High Latitudes category	Usage other than in ScenarioMIP
~~SSP1-1.9~~ SSP1-19	0.012	0.011	Low	Medium	High	
~~SSP1-2.6~~ SSP1-26	0.013	0.009	Low	Medium	High	
~~SSP2-4.5~~ SSP2-45	0.019	0.015	Medium	High	Medium	DCPP, MiKlip
~~SSP3-low~~ SSP3-LowNTCF	0.018	0.017	Medium	High	Medium	
~~SSP3-ref~~ SSP3-70	0.031	0.027	High	High	Medium	
~~SSP4-3.4~~ SSP4-34	0.020	0.020	Medium	Low	High	
~~SSP4-6.0~~ SSP4-60	0.030	0.026	High	Low	Medium	
~~SSP5-3.4~~ SSP5-34-OS	0.018	0.012	Medium	Medium	Low	
~~SSP5-ref~~ SSP5-85	0.028	0.022	High	Medium	Low	RFMIP, HighResMIP

Table 3. Mid-2090s anthropogenic aerosol SW (E)RF at TOA from MACv2-SP as long-term averages +/- year-to-year standard deviation in Wm^{-2}.

Year	Scenario	Clear-sky RF	All-sky RF	Clear-sky ERF	All-sky ERF
mid-2000s	Historical	-0.656 +/- 0.001	-0.599 +/- 0.003	-0.67 +/- 0.07	-0.50 +/- 0.32
mid-2090s	~~SSP1-2.6~~ SSP1-26	-0.239 +/- 0.0003	-0.204 +/- 0.002	-0.24 +/- 0.07	-0.15 +/- 0.28
	~~SSP3-ref~~ SSP3-70	-0.678 +/- 0.001	-0.568 +/- 0.005	-0.69 +/- 0.06	-0.54 +/- 0.29
	~~SSP5-ref~~ SSP5-85	-0.463 +/- 0.001	-0.327 +/- 0.006	-0.45 +/- 0.06	-0.33 +/- 0.27
mid-2090s	~~SSP1-2.6-LBG~~ SSP1-26-LBG	-0.239 +/- 0.0003	-0.388 +/- 0.002	-0.26 +/- 0.07	-0.39 +/- 0.29
	~~SSP3-ref-LBG~~ SSP3-70-LBG	-0.678 +/- 0.001	-1.020 +/- 0.006	-0.69 +/- 0.07	-0.92 +/- 0.28
	~~SSP5-ref-LBG~~ SSP5-85-LBG	-0.463 +/- 0.001	-0.644 +/- 0.005	-0.47 +/- 0.06	-0.56 +/- 0.28